AEDC-TR-73-21

EFFECTS OF NOZZLE GEOMETRY AND DIAPHRAGM LOCATION ON THE STARTING PROCESS IN A LUDWIEG TUBE

Leo T. Smith and Francis Mosnier

Yale University

February 1973

ARNOLD ENGINEERING DEVELOPMENT CENTER
AIR FORCE SYSTEMS COMMAND
ARNOLD AIR FORCE STATION, TENNESSEE

NOTICES

When U. S. Government drawings specifications, or other data are used for any purpose other than a definitely related Government procurement operation, the Government thereby incurs no responsibility nor any obligation whatsoever, and the fact that the Government may have formulated, furnished, or in any way supplied the said drawings, specifications, or other data, is not to be regarded by implication or otherwise, or in any manner licensing the holder or any other person or corporation, or conveying any rights or permission to manufacture, use, or sell any patented invention that may in any way be related thereto.

Qualified users may obtain copies of this report from the Defense Documentation Center.

References to named commercial products in this report are not to be considered in any sense as an endorsement of the product by the United States Air Force or the Government.

EFFECTS OF NOZZLE GEOMETRY AND DIAPHRAGM LOCATION ON THE STARTING PROCESS IN A LUDWIEG TUBE

Leo T. Smith and Francis Mosnier
Yale University

FOREWORD

The work reported herein was sponsored by the Arnold Engineering Development Center (AEDC), Air Force Systems Command (AFSC), Arnold Air Force Station, Tennessee, under Program Element 65802F. Technical monitoring of the contract was performed by Capt Carlos Tirres, USAF, Research and Development Division, Directorate of Technology.

The effort was conducted from July 1971 through June 1972 at Yale University under Contract F40600-70-C-0008. The manuscript was submitted for publication in August 1972.

The authors are indebted to the principal investigator, Professor Peter P. Wegener, for assistance and many helpful discussions. Further thanks go to Dr. Dominic J. Cagliostro for suggestions and help during the initial phase of this investigation. The uniform flow nozzles used here were based on a design provided by Mr. Robert L. P. Voisinet of the U. S. Naval Ordnance Laboratory. Further thanks are extended to the U. S. Naval Ordnance Laboratory for loaning us the Zeiss Mach-Zehnder Interferometer which was used in many of the experiments.

The reproducibles used in the reproduction of this report were supplied by the authors.

This technical report has been reviewed and is approved.

CARLOS TIRRES
Captain, USAF
Research & Development Division
Directorate of Technology

ROBERT O. DIETZ
Director of Technology

ABSTRACT

The starting process in the Ludwieg tube, an intermittent type tube wind tunnel, was experimentally investigated. Starting flow with varying initial supply gas pressure, nozzle geometry, and downstream diaphragm location, was studied. Two types of closed jet nozzle configurations were used: uniform flow M = 1.6 nozzles, and wedge type M = 1.6 nozzles. Dry air at 1, 2, and 3 atm pressure and room temperature served as the test gas. Starting times were determined from static pressure recordings, made at the exit of the nozzle, and the presence or absence of starting shock waves was confirmed by high speed shadowgraph films of the flow. A dimensional analysis that relates nozzle starting time to the supply conditions, nozzle inlet angle, nozzle contraction ratio, and distance to the diaphragm was performed, and it was found to correlate the measurements. For all combinations of supply conditions, nozzle geometry, and diaphragm location treated, starting shock waves were observed in the nozzle. These shocks were eliminated and steady supersonic flow was established smoothly throughout the closed jet nozzle by applying boundary layer suction at the exit.

CONTENTS

NOMENCLATURE

A	area
a	velocity of sound
C_1, C_2	constants appearing in Equation (8)
D_n	constants appearing in Equation (10), n = 0,1,2,3
d	suction slit dimension
F	force
L	length
ℓ	characteristic nozzle length measured from nozzle inlet to nozzle exit
M	mass; Mach number
p	pressure
R	radius of curvature
T	time; temperature
t_i	total starting time
t_{il}	time to establish sonic flow in nozzle throat
t_T	total time of steady supersonic flow
t_s	measured starting time
w	nozzle width
x	distance coordinate
y	distance coordinate
α	nozzle inlet angle
γ	ratio of specific heats
λ	distance between nozzle exit and diaphragm location
ρ	density
μ	dynamic viscosity

SUBSCRIPTS

1	initial conditions in low pressure tube
4	initial conditions in high pressure tube
e	indicates property at the nozzle exit
s	supply tube

SUPERSCRIPTS

*	indicates property at the nozzle throat

ILLUSTRATIONS

I

INTRODUCTION

For vehicles that fly at transonic and moderate supersonic speeds ($0.8<M<3$), present and future testing facilities must be capable of simulating free flight Reynolds numbers of at least 10^9 (e.g., Refs. 1-3). One device, the intermittent tube-wind-tunnel, originally conceived by H. Ludwieg (4) in 1955, is remarkably well suited to this kind of application. Indeed, when compared to conventional continuous and blowdown wind tunnels, the Ludwieg tube now appears to be the only device capable of economically meeting high Reynolds number requirements (1).

As is the case with the Yale University Ludwieg tube (Refs. 5-7), the tunnel may consist of a conventional shock tube modified by the insertion of a converging-diverging nozzle into the section upstream of the diaphragm (high pressure section).* The operating stages of this configuration are shown in Figure 1, an x-t diagram and sketch of the tube. When the diaphragm is broken at time zero, a shock wave followed by a contact surface travels downstream into the low pressure gas. Upstream of the diaphragm, an expansion wave propagates into the high pressure gas, accelerating it toward the nozzle. At time t_{i_1}, flow at the nozzle throat becomes sonic, and the remaining part of the expansion fan is swept downstream, the last disturbance leaving the exit of the nozzle at time t_i, the starting time of the tube. There follows in the nozzle a steady supersonic flow of short**, but useful, duration, t_T, which lasts until the expansion wave reflects from the end wall of the supply tube and returns to the nozzle inlet. During steady flow, a high stagnation pressure (typically 95% of the initial supply tube pressure) is maintained at the inlet of the nozzle without the use of special control valves. Since Reynolds number increases directly with stagnation pressure, high Reynolds numbers, limited only by the maximum allowable stress on tube walls, model supports, etc., are possible.

* Current and proposed designs vary. Flow may be initiated either by breaking a diaphragm or activating a quick opening valve upstream or downstream of the nozzle. The nozzle and test section may open into a large, pre-evacuated dump tank, or, as in the case of Ludwieg's original design (4), directly to the atmosphere.

** It is recalled that an expansion wave propagates into a gas at rest at the speed of sound (~1000 ft/sec at room temperature). Thus, the running time of the tunnel is roughly 2 msec per foot of supply tube length.

Steady flow conditions in the nozzle and, therefore, steady state loads on models and supports can be accurately computed from equations derived in the literature. In these analyses, it is generally assumed that the nozzle has zero length, and that one is dealing with the one-dimensional, inviscid flow of a perfect gas (e.g., Refs. 8 and 9). The interest here, however, is in the starting stage, i.e., the elapsed time between the rupture of the diaphragm and the establishment of steady supersonic flow in the test section of the nozzle. While conditions during the starting process can be calculated using the method of characteristics for inviscid, quasi - one-dimensional, unsteady flow (Refs. 10 and 11), measured values tend to differ significantly from those computed; this is due, in part, to two-dimensional and viscous effects. The situation is further complicated by the presence of starting shock waves in the diverging part of nozzles operated in a closed-jet configuration (Refs. 12 and 13). Such shocks appear to result from complicated wave interactions and boundary layer thickening, and they travel downstream through the nozzle prior to the steady flow stage. Recent studies have shown that nozzles run in a semi-open jet configuration do not exhibit starting shocks (Refs. 7 and 13), and point to the importance of nozzle and test section geometry in determining flow conditions during the starting stage.

In this report, the results of systematic experimental investigations into the effects of nozzle geometry on the starting times, and the appearance of starting shock waves in nozzles run in a closed jet configuration are presented. The research effort is divided into the following three phases:

1) Determine those nozzle parameters that influence the starting time by performing a dimensional analysis of the problem. Based on this analysis, only three variables are considered : nozzle inlet geometry, specifically the inlet angle α† nozzle contraction ratio A_s/A^* (ratio of supply tube cross section area to nozzle throat area); and the distance λ, between the nozzle exit and the downstream diaphragm location.

2) Design a series of nozzles and quantitatively determine nozzle starting time as a function of the above-mentioned variables.

3) Carry out a series of boundary layer suction experiments in an attempt to reduce the boundary layer thickness and flow separation during the starting stage and thereby eliminate starting shock waves.

---

† Note symbol index on page v.

II

DIMENSIONAL ANALYSIS

As previously stated, the analytic approach does not yield reliable predictions of the flow process during the starting stage. For the problem at hand, an alternate procedure is adopted which begins with a dimensional analysis. While this is no substitute for a solution to the unsteady equations of motion, this method will serve as a guide to designing experiments, and analyzing the results obtained.

The unsteady flow of a thermally and calorically perfect gas (dry air) with constant ratio of specific heats, γ, equal to 1.4 is considered here. Previous work done (Refs. 7 and 13) has shown a dependence of starting time on the initial gas conditions in the supply tube, and this fact is incorporated in the current analysis. Referring to the notation of Figure 2, the initial supply gas properties and the geometry of the nozzle are described by the following variables:

p_4 - initial supply pressure†

ρ_4 - initial supply density†

μ_4 - initial supply dynamic viscosity

γ - ratio of specific heats

ℓ - characteristic nozzle length measured from nozzle inlet to nozzle exit

λ - distance between nozzle exit and diaphragm location

A_s - supply tube area

A^* - nozzle throat area

A_e - nozzle exit area

dA/dx - change in area with respect to distance measured along the center-line of the nozzle

It is now stipulated that the starting time t_s, is related to the above variables through a general equation of the form

$$t_s = f_1(p_4, \rho_4, \mu_4, \gamma, \ell, \lambda, A_s, A^*, A_e, dA/dx) \quad . \qquad (1)$$

† Since a perfect gas is considered, the combinations (p_4, T_4) or (ρ_4, T_4) could equally be chosen, where T_4 would be the initial temperature of the supply gas.

In all, there are 11 variables relating to this problem, involving three dimensions, L, length, M, mass (or F, force), and T, time. From Buckingham's theorem, it is expected to find 11 - 3 = 8 so called π-terms, or dimensionless groups of variables to fully describe the flow. Formation of these groups by the standard methods employed in dimensional analysis yields the following general expression for the nondimensional starting time

$$\frac{t_s}{\ell}\sqrt{\gamma \frac{p_4}{\rho_4}} = f_2 \left[\frac{\ell \rho_4}{\mu_4} \sqrt{\gamma \frac{p_4}{\rho_4}}, \frac{1}{\ell} \frac{dA}{dx}, \frac{A_s}{A^*}, \frac{A_e}{A^*}, \frac{\lambda}{\ell}, \frac{A^*}{\ell^2}, \gamma \right] \quad . \quad (2)$$

Equation (2) may be further simplified by introducing the speed of sound

$$a_4 = \sqrt{\gamma \frac{p_4}{\rho_4}} \quad ,$$

and noting that the exit Mach number, M_e, is a function of A_e/A^*. In addition, γ is omitted since it will remain constant in all cases considered here. Thus,

$$\frac{t_s a_4}{\ell} = f_3 \left[\frac{a_4 \rho_4 \ell}{\mu_4}, \frac{1}{\ell} \frac{dA}{dx}, \frac{A_s}{A^*}, M_e, \frac{\lambda}{\ell}, \frac{A^*}{\ell^2} \right] \quad . \quad (3)$$

Two of the dimensionless groups appearing in Equation (3), $a_4 \rho_4 \ell / \mu_4$ and $(1/\ell)\, dA/dx$, are somewhat unusual in their interpretation. The former is in the form of a Reynolds number (i.e., a ratio of inertial to viscous forces) based on the initial gas conditions in the supply, and may be thought of as the Reynolds number associated with the propagation of the head of the expansion fan upstream through the nozzle. It is directly related to the conventional Reynolds number, based on steady flow conditions in the nozzle test section, through the standard gasdynamic equations for Ludwieg tube operation (8) and one-dimensional nozzle flow (e.g., Ref. 14). For experiments carried out at the same supply tube temperature (as is the case here), $a_4 \rho_4 \ell / \mu_4$

varies directly with supply pressure, and may be regarded as a measure of the pressure, or Reynolds number (see p. 2) effects on the starting process. In plotting experimental results, it is convenient to substitute the supply pressure, p_4, for this group.

Since dA/dx is in general a function of distance along the nozzle, it appears that $(1/\ell)\, dA/dx$ could not be held constant (as is necessary, e.g., to isolate the effect of varying contraction ratio, A_s/A^*). Here, nozzles having similar geometry in the throat and supersonic sections, but with varying inlet geometry are used. For a straight wall inlet section, with inlet angle α (see Figure 2), $(1/\ell)\, dA/dx$ is then replaced by

$$\frac{1}{\ell}\frac{dA}{dx} = \frac{2w}{\ell}\frac{dy}{dx} = \frac{2\ w\ \tan(\alpha)}{\ell},$$

where w is the width of the nozzle. Finally, all experiments will be carried out with M_e held constant and† $A^*/\ell^2 \ll 1$.

Under the above restrictions, Equation (3) becomes

$$\frac{t_s a_4}{\ell} = f_4\left[\frac{a_4 \rho_4 \ell}{\mu_4},\ \frac{2\ w\ \tan(\alpha)}{\ell},\ \frac{A_s}{A^*},\ \frac{\lambda}{\ell}\right] . \qquad (4)$$

In Equation (4) the supply conditions, inlet angle, contraction ratio, and downstream diaphragm location each appear in a single nondimensional group. Thus by carrying out experiments in which three of these groups are held constant, nondimensional starting time is determined as a function of the fourth. The validity of this analysis and experimental approach depends, of course, on the success to which experimental results can be correlated using the nondimensional groups of Equation (4). That this is the case here will be shown in the experiments described below.

---

† In all cases studied here, $A^*/\ell^2 \leq 0.06$.

III

EXPERIMENTAL APPARATUS

The Yale University Ludwieg tube† is sketched in Figure 3. Two sections immediately upstream and downstream of the test section respectively produce a smooth transition from the circular supply and dump tubes to the rectangular, 1.5 ft test section. Two-dimensional nozzles are mounted in the test section such that the nozzle exit is in the center of the 4 in. diameter viewing area. The windows used are of high quality optical glass, and one of these may be replaced by an aluminum insert for mounting a fast response-time quartz pressure transducer at the exit of the nozzle. Extension blocks for each nozzle are inserted between the nozzle exit and the end of the test section to form a closed jet configuration. Also shown in Figure 3, but not used in this investigation, is a 17 cu ft dump tank, which may be used to eliminate reflected shock waves and to provide a large vacuum chamber for boundary layer suction experiments.

Three downstream diaphragm positions were used in this investigation, located at λ = 12.7, 377, and 821 cm (0.42, 12.4, and 26.9 ft). In the case of the farthest downstream location, the tube is exhausted directly to the atmosphere and we have an initial pressure ratio across the diaphragm of $p_4/p_1 = 3$, with p_4 = 3 atm. Experiments using the other two locations were carried out with $p_4/p_1 = 10$, and p_4 = 1, 2, and 3 atm. The operating gas was dry air in all cases, and several sheets of 0.002 in. thick cellophane provided diaphragms with breaking times of less than 0.1 msec (13).

Two sets of nozzles were tested:

1) A set of four uniform flow nozzles††, with inlet angles α = 20°, 30°, 50°, and 67° respectively, and constant contraction ratio and exit Mach number (A_s/A^* = 22, M_e = 1.6). All nozzles in this set were geometrically similar in the throat and supersonic region. Specific dimensions are given in Table 1, and are shown in Figure 4A for the 30° inlet angle nozzle.

2) A set of four wedge-type nozzles, with contraction ratios A_s/A^* = 5, 8, 12, and 16 respectively. These nozzles

---

† A brief description of this facility is given here. Full details of the tube wind tunnel and auxiliary equipment may be found in Refs. 5-7.

†† The supersonic section of these nozzles was designed by Mr. Robert L.P. Voisinet of the U.S. Naval Ordnance Laboratory.

are designed with a three-degree half angle expansion, a 2.5 in. radius of curvature at the throat, and a 30° inlet angle. Exit Mach number is 1.6 for each nozzle. Table 1 and Figure 4B show specific nozzle dimensions for this set. Both the nozzles and extension blocks were machined from plexiglass, and they completely spanned the 2 in. wide test section. Surfaces exposed to the flow were polished free of scratches, tool marks, etc.

The nozzle and extension blocks used in the boundary layer suction experiments are shown in Figure 5. This is a uniform flow nozzle, geometrically similar to those of set 1 above (with $A_s/A^* = 22$ and $M_e = 1.6$), but with a more complicated inlet geometry. A 1.75 in. wide suction slit is located perpendicular to the flow direction at the exit of the upper and lower nozzle block. These slits connect directly to a rectangular channel cut in the extension blocks, and these channels in turn empty into the low pressure dump tube. The part of the initial expansion fan that enters the channel reflects off the end of the nozzle block. This creates a lower pressure in each channel than exists in the exit of the nozzle, thereby producing suction through the slits for boundary layer reduction during the starting stage.

The tunnel is instrumented with a pressure measuring system, a photographic system used in conjunction with a Mach-Zehnder Interferometer†, and a supporting electronic system (see Figure 3). Starting times were determined from static pressure vs. time recordings made at the exit of each nozzle using a calibrated, 3 μsec rise-time quartz pressure transducer (Kistler, Model #606L). Additional pressure measurements were made to check nozzle supply conditions in the supply tube. The presence or absence of starting shock waves was determined from high speed movie shadowgraphs with a 0.2 msec frame to frame sampling rate. Shadowgraph films were taken using a Fastax 16 mm Model WF3 motion picture camera with a film speed of approximately 5000 frames per second.

---

† The authors are grateful to the U.S. Naval Ordnance Laboratory for loaning them this instrument.

IV

EXPERIMENTAL RESULTS

The starting time of each nozzle is determined from direct measurement of the static pressure history at the exit. This is illustrated for two different nozzles (one uniform flow, and one wedge-type) in the pressure-time oscilloscope traces shown in Figure 6. The starting point of the time scale roughly coincides with rupture of the diaphragm. Measured starting time, t_s, is taken to be

$$t_s = t_2 - t_1 \quad , \tag{5}$$

where t_1 is the time at which the expansion wave arrives at the exit, and t_2 is the time at which constant pressure is established there. Note that t_s is not the total starting time, t_i, as defined in Figure 1. In this case

$$t_i = t_s + t_1 \quad , \tag{6}$$

however, t_s is most sensitive to changes in the nozzle geometry, while t_1 is given approximately by λ/a_4. Therefore, t_s will be the starting time of interest in this work.

In the uniform flow nozzles, static pressure gradually approaches a constant value (Figure 6), and a point can be chosen arbitrarily at which the pressure has fallen to within 10% of its steady flow value in determining t_s. This pressure difference, i.e., ±5%, also represents the accuracy with which pressure can be measured off the oscilloscope trace. A slight pressure undershoot, measured to be less than 5% of the steady flow pressure in all cases occurs in the wedge type nozzles. In these cases, the point at which the static pressure first reaches its steady flow value is used to determine the starting time. Starting times are measured in each nozzle for supply pressures p_4 = 1 and 2 atm, and diaphragm locations λ = 12.7 and 377 cm. An initial pressure ratio p_4/p_1 = 10 insures fully developed supersonic flow in the nozzle, and dry air is used in all experiments, with initial supply temperature T_4 = 24 ± 1°C. Additional results are obtained for one wedge nozzle with contraction ratio 12 at all three diaphragm locations (12.7,

377, and 821 cm). For this case, p_4 = 3 atm and p_4/p_1 = 3, with the tube exhausting directly into the atmosphere for the farthest diaphragm location.

Measured starting times are plotted against nozzle inlet angle for constant contraction ratio A_s/A^* = 22, in Figure 7. Each point represents the arithmetic mean of several experimental results, with the high and low values indicated by the error bars. Starting time is seen to decrease with increasing inlet angle, and a strong effect of diaphragm location is noted, with starting times being nearly double at the far downstream position. Starting time is also seen to increase with initial supply pressure or, equivalently, nozzle Reynolds number. Here, the Reynolds number per unit length at the exit is 5×10^6 ft^{-1} and 1×10^7 ft^{-1} for p_4 = 1 atm and 2 atm respectively.

At this point, recall the result of the dimensional analysis (Equation 4) which for constant p_4, λ/ℓ, and A_s/A^* yields

$$\frac{t_s a_4}{\ell} = f_5 \left[\frac{2 w \tan(\alpha)}{\ell} \right] \quad . \tag{7}$$

Nondimensional starting times are shown in Figure 8, and the trend of the results indicates a linear form for Equation (7), i.e.,

$$\frac{t_s a_4}{\ell} = C_1 + C_2 \left[\frac{2 w \tan(\alpha)}{\ell} \right] \quad , \tag{8}$$

Constants C_1 and C_2 determined by the least square method, using all of the available results, are listed in Table II. At the near diaphragm position, the correlation is excellent, with the mean values of $t_s a_4/\ell$ deviating by less than 1% from the fitted line. At λ = 377 cm, there is increased scatter in the data, with a maximum deviation of 9% occurring at $2 w \tan(\alpha)/\ell = 0.94$ ($\alpha = 50°$).

The results of varying nozzle contraction ratio while maintaining a constant inlet angle of 30° are shown in Figure 9, where the mean value of the starting time is plotted. The spread in the data, i.e., the high and low

values of several results at the same contraction ratio, falls within the plotted symbol in all cases. A smooth curve is drawn by eye through the data points, with the dashed section between A_s/A^* = 16 and 22 indicating a change from wedge type to uniform flow nozzle geometry. A decreased dependence of starting time on Reynolds number is noted at low contraction ratios (for fixed supply tube area, a lower contraction ratio corresponds to increased throat area). Again the strong influence of diaphragm location is evident. Minimum values of the starting time occur at A_s/A^* = 12.

Nondimensional starting time is plotted as a function of contraction ratio in Figure 10. With p_4, α, and λ held constant it is expected that the results will fit a relation of the form

$$t_s a_4/\ell = f_6 (A_s/A^*) \quad . \tag{9}$$

No simple algebraic form for Equation (9) relates the results; however a cubic expression of the form

$$\frac{t_s a_4}{\ell} - C_2 \left[\frac{2\ w\ \tan(\alpha)}{\ell}\right] = \sum_{n=0}^{3} D_n \left(\frac{A_s}{A^*}\right)^n \tag{10}$$

correlates the combined results of both the uniform flow and wedge type nozzles. This is illustrated for λ = 12.7 cm and p_4 = 1 atm and 2 atm in Figures 11 and 12 respectively, and values of the constants, D_n, are given in Table III. Agreement between the experimental points and the fitted curve is good, with a maximum deviation of 5% at A_s/A^* = 5. (Here, C_2 is the constant previously obtained from the results with uniform flow nozzles with contraction ratio A_s/A^* = 22. For A_s/A^* = 22, the right-hand side of Equation (10) reduces to the constant C_1 of Equation (8).) It should be noted that Equation (10) applies only over the range of parameters investigated, and does not lend itself to extrapolation beyond those values of A_s/A^* reported here.

The variation of measured nondimensional starting time with diaphragm location, λ/ℓ, for constant p_4 = 3 atm, α = 30°, and A_s/A^* = 12, is shown in Figure 13. It is seen that the starting time increases linearly with the

distance between nozzle exit and diaphragm location.

In addition to the above starting time measurements, high speed shadowgraph movies of the entire flow process were taken for each nozzle with p_4 = 1 and 2 atm, and λ = 12.7 and 377 cm. In all cases investigated, starting shock waves are observed ahead of the nozzle exit, in agreement with the previous closed jet experiments of Cagliostro (13). Further evidence of the appearance of starting shock waves is found in the oscilloscope traces shown in Figure 6. Here, the abrupt change of slope occurring approximately one third of the way into the starting stage indicates passage of the starting shock through the exit. Estimates of the time at which the starting shock sweeps by the exit, obtained from the high speed movies, roughly confirm this result.

The effects of boundary layer suction on the flow during the starting stage are evident from the experiments with the Mach 1.6 nozzle and extension block combination sketched in Figure 5. Figure 14 shows prints of film strips from high speed shadowgraph movies of the starting process with and without suction. Flow is from left to right, and the time elapsed between each frame is about 0.2 msec. The nozzle exit and location of the suction slits is in the center of the field of view, while the throat of the nozzle is located at the left-hand edge of the picture. Without suction (print A), a starting shock wave is observed ahead of the exit. It moves downstream with time, sweeping past the exit and eventually out of the nozzle and into the dump tube. Upstream of the shock wave the flow is steady. Print B shows the starting process with suction. Here, the dimensions of the slit are 1.75" x 0.120", with the long side placed perpendicular to the flow direction. A starting shock wave does not form ahead of the exit in this case. Instead, pressure disturbances originate at the slit location and move downstream out of the nozzle as steady flow is established.

A series of such experiments was carried out using the same nozzle at p_4 = 1 and 2 atm, and with suction slit dimensions ranging from 1.75" x 0.015" to 1.75" x 0.200". In all cases investigated, starting shock waves do not occur when suction is applied to the boundary layer, whereas, under the same supply conditions, but without suction, such shocks are observed.

Static pressure histories of the starting flow with and without suction are presented in Figures 15 and 16 for p_4 = 1 atm and 2 atm respectively. Without suction, an abrupt change in slope is observed, occurring at a time roughly coinciding with the arrival of the starting shock at the exit, as determined from high speed movies. Increasing the area of

the suction slits tends to "smooth out" the pressure behavior during starting. This is evident in Figures 17 and 18, where the measured static pressure at the exit, p_e, is plotted as a function of time. Time zero starts with the arrival of the expansion wave at the exit, and the ordinate is made dimensionless by dividing by the initial supply pressure, p_4. At p_4 = 1 atm, data points obtained using the largest slit area can be connected by a smooth curve. With suction a slight pressure undershoot occurs, but suction has little or no effect on the value of the final steady pressure. In addition, suction produces a slight decrease in the starting time of the nozzle.

V

DISCUSSION OF RESULTS

For the flow conditions and nozzles used in this investigation, it has been shown that nozzle geometry, diaphragm location, and supply conditions have a significant effect on the starting process. Each of these parameters is isolated in a single dimensionless group as seen in Equation (4). Although no single empirical equation predicting the overall behavior of the starting time has been produced, the dimensionless groups of Equation (4) successfully correlate the results. Thus, at fixed contraction ratio, diaphragm location, and supply pressure, nondimensional starting time is linearly proportional to the nondimensional inlet angle as demonstrated in Figure 7. The empirical relation given by Equation (10) relates the influence of inlet angle and contraction ratio on starting time for a given supply condition and diaphragm location. An interesting feature here is the minimum starting time observed at $A_s/A^* = 12$. Bearing in mind that Equation (10) is based solely on experimental results, there appears to be no fundamental physical reason to suggest this form of relation.

The most striking result obtained is the strong linear dependence of starting time on the distance between the nozzle exit and the diaphragm location. As seen in Figure 13, increasing this distance by a factor of 2 nearly doubles the starting time. This behavior is to be expected when the propagation of the expansion fan toward the nozzle is considered. As is well known, an expansion wave traveling along a tube spreads out with time (see Figure 1). Thus, a nozzle located far from the diaphragm will require a longer time to experience an equivalent drop in pressure than that required for a nozzle located nearer to the diaphragm. Such considerations are of importance in the design of Ludwieg tubes. Since total operating time is fixed by the length of the supply section, starting time must be minimized in order to provide sufficient time to record data during the steady flow period. As shown here, this can be accomplished by positioning the diaphragm immediately downstream of the nozzle.

All combinations of supply pressure, nozzle geometry, and diaphragm location resulted in starting shock waves in the closed jet nozzles. Such shocks increase the transient forces on a model during tunnel starting and thereby raise the design requirements of a model and its support. Based on the suggestion that starting shocks result from boundary layer thickening and flow separation during start-up (Refs. 12 and 13), boundary layer suction was applied at the exit of the nozzle. This technique is seen to eliminate starting

shock waves upstream of the exit, but pressure disturbances do originate at the suction slits. Since models would be positioned at the exit, it is suggested that suction be applied downstream of the exit in the closed jet portion of the nozzle. Although further experimental work is indicated in this area, it is evident that steady supersonic flow can be established smoothly without the formation of starting shock waves while still retaining the closed jet configuration.

VI

SUMMARY

Measured flow properties differ considerably from current theoretical predictions of the starting flow in a supersonic Ludwieg tube wind tunnel. The present approach to this problem is through dimensional analysis. Under the restriction of constant Mach number, M = 1.6, and with a perfect gas (air), it is found that five dimensionless groups of variables relate starting time to the nozzle inlet angle, nozzle contraction ratio, downstream distance to the diaphragm, and initial supply gas properties or, equivalently, the Reynolds number in the nozzle. Using this dimensionless representation, it is possible to correlate measured starting time to each of the above variables although no general empirical equation involving all parameters is achieved.

In terms of the present nondimensional representation, the experimental results show the following:

(1) At constant contraction ratio, nondimensional starting time is linearly proportional to the nondimensional inlet angle, it increases slightly with increased supply pressure (and therefore, increased Reynolds number).

(2) At constant inlet angle, nondimensional starting time is not a simple algebraic function of contraction ratio. Instead a cubic expression of the form

$$\sum_{n=0}^{3} D_n \left(\frac{A_s}{A^*}\right)^n$$

represents the data, with a minimum starting time at $A_s/A^* = 12$. Note that this expression arises solely from the experimental results presented here and is not based on physical reasoning. Neither does it lend itself to extrapolation beyond the conditions investigated here.

(3) As expected, starting time increases with distance to the downstream diaphragm location. This is the major effect found in this study, with an increase in distance by a factor of two resulting in nearly double the starting time. This result is of obvious importance in the design of future Ludwieg tube facilities.

All combinations of nozzle geometry, supply conditions, and diaphragm positions tested here resulted in the formation of starting shock waves in the closed jet nozzle. By applying suction to the boundary layer during the start, the starting shock is eliminated, and pressure behavior during the starting flow is considerably improved. Although this method requires further investigation, especially in the positioning of suction slits along the nozzle, the results indicate that steady supersonic flow can be established smoothly throughout the nozzle, without the formation of starting shock waves, while still retaining the closed jet configuration.

REFERENCES

1. Enkenhus, K. R. and Merritt, D. L., "Evaluation of Two Types of Facilities to Fulfill the Need for High Reynolds Number Transonic Testing", U. S. Naval Ordnance Laboratory, Report No. NOLTR 71-147, July 1971.

2. Fila, L. J., "Preliminary Considerations in the Design of a Ludwieg Tube for High Reynolds Numbers", Arnold Engineering Development Center, Report No. AEDC-TR-67-210, February 1968.

3. Falk, T. J., "A Tube Wind Tunnel for High Reynolds Number Supersonic Testing", Office of Aerospace Research, U.S.A.F. Report No. ARL 68-0031, February 1968.

4. Ludwieg, H., "Der Rohrwindkanal", Zeitschrift für Flugwissenschaft, Jahrgang 3, Heft 7, July 1955, pp. 206-216; also Ludwieg, H., "Tube Wind Tunnel: A Special Type of Blow-down Tunnel", AGARD Rept. 143, July 1957, NATO Headquarters, Scheveningen, Holland.

5. Wegener, P. P. and Buzyna, G., "Experiments on Shock Stand-off Distance in Non-equilibrium Flow", Journal of Fluid Mechanics, Vol. 37, Pt. 2, June 1969, pp. 325-335.

6. Johnson, J. A., III and Cagliostro, D., "Experiments with a Supersonic Tube Wind-Tunnel", Arnold Engineering Development Center, Final Report No. AEDC-TR-70-71. March 1970.

7. Johnson, J. A., III and Cagliostro, D., "Starting Phenomena in a Supersonic Tube Wind Tunnel", AIAA Journal, Vol. 9, No. 1, January 1971, pp. 101-105.

8. Cable, A. J. and Cox, R. N., "The Ludwieg Pressure Tube Supersonic Wind Tunnel", The Aeronautical Quarterly, Vol. XIV, Pt. 2, May 1963, pp. 143-157.

9. Becker, E., "Grenzschichteffekte beim Rohrwindkanal", Jahrbuch der Wissenschaftliche Gesellschaft für Luftfahrt, January 1957, WGL-Tagung Essen. Germany, pp. 232-237.

10. Warmbrod, J. D. and Struck, H. G., "Application of the Characteristic Method in Calculating Time Dependent, One Dimensional, Compressible Flow in a Wind Tunnel", NASA TM X-53769, August 1968.

11. Warmbrod, J. D., "A Theoretical and Experimental Study of Unsteady Flow Processes in a Ludwieg Tube Wind Tunnel", NASA TN D-5469, November 1969.

12. Bull, G. V., "Investigation into the Operating Cycle of a Two-Dimensional Supersonic Wind Tunnel", Journal of Aeronautical Sciences, Vol. 19, No. 9, September 1952, pp. 609-614.

13. Cagliostro, D., "Experiments on the Starting Process in a Ludwieg Tube", Arnold Engineering Development Center, Report No. AEDC-TR-72-42, March 1972.

14. Liepmann, H. W. and Roshko, A., Elements of Gasdynamics, John Wiley, New York, 1957.

TABLE I

Characteristic dimensions of uniform flow and wedge-type nozzles

A. Uniform flow nozzles

Nozzle #	α°	ℓ cm	2 w tan(α)/ℓ	A^*/ℓ^2
1	20	20.8	0.179	0.015
2	30	15.7	0.373	0.026
3	50	12.9	0.937	0.039
4	67	10.4	2.500	0.060

Common dimensions - $A_s/A^* = 22$; $A^* = 6.45$ cm^2; w = 5.08 cm; $R^* = 25.4$ cm; $M_e = 1.6$

B. Wedge nozzles

Nozzle #	A_s/A^*	ℓ cm	2 w tan(α)/ℓ	A^*/ℓ^2
6	16	15.5	0.379	0.037
7	12	16.4	0.368	0.044
8	8	18.2	0.323	0.054
9	5	21.4	0.274	0.062

Common dimensions - α = 30°; w = 5.08 cm' $R^* = 6.35$ cm; $M_e = 1.6$.

TABLE II

Measured nondimensional starting time as a function of nondimensional nozzle inlet angle

$$\frac{t_s a_4}{\ell} = C_1 + C_2 \left[\frac{2\ w\ \tan(\alpha)}{\ell}\right]$$

p_4 atm	λ cm	C_1	C_2
1.0	12.7	10.9	0.74
2.0	12.7	12.7	1.53
1.0	377	18.9	5.13
2.0	377	21.8	5.80

$T_4 = 24°C$

$a_4 = 346$ m/sec

$w = 5.08$ cm

$20° \leq \alpha \leq 67°$

$A_s/A^* = 22$

10 cm $\leq \ell \leq$ 21 cm

TABLE III

Measured nondimensional starting time as a function of nondimensional nozzle inlet angle and nozzle contraction ratio

$$t_s a_4/\ell - C_2 \left[2 w \tan(\alpha)/\ell\right] = D_0 + D_1(A_s/A^*) + D_2(A_s/A^*)^2 + D_3(A_s/A^*)^3$$

p_4 atm	λ cm	C_2	D_0	D_1	D_2	D_3
1.0	12.7	0.74	4.91	0.52	-0.10	0.004
2.0	12.7	1.53	3.50	0.97	-0.15	0.006

T_4 = 24°C

a_4 = 346 m/sec

w = 5.08 cm

$20° \leq \alpha \leq 67°$

$5 \leq A_s/A^* \leq 22$

10 cm $\leq \ell \leq$ 21 cm

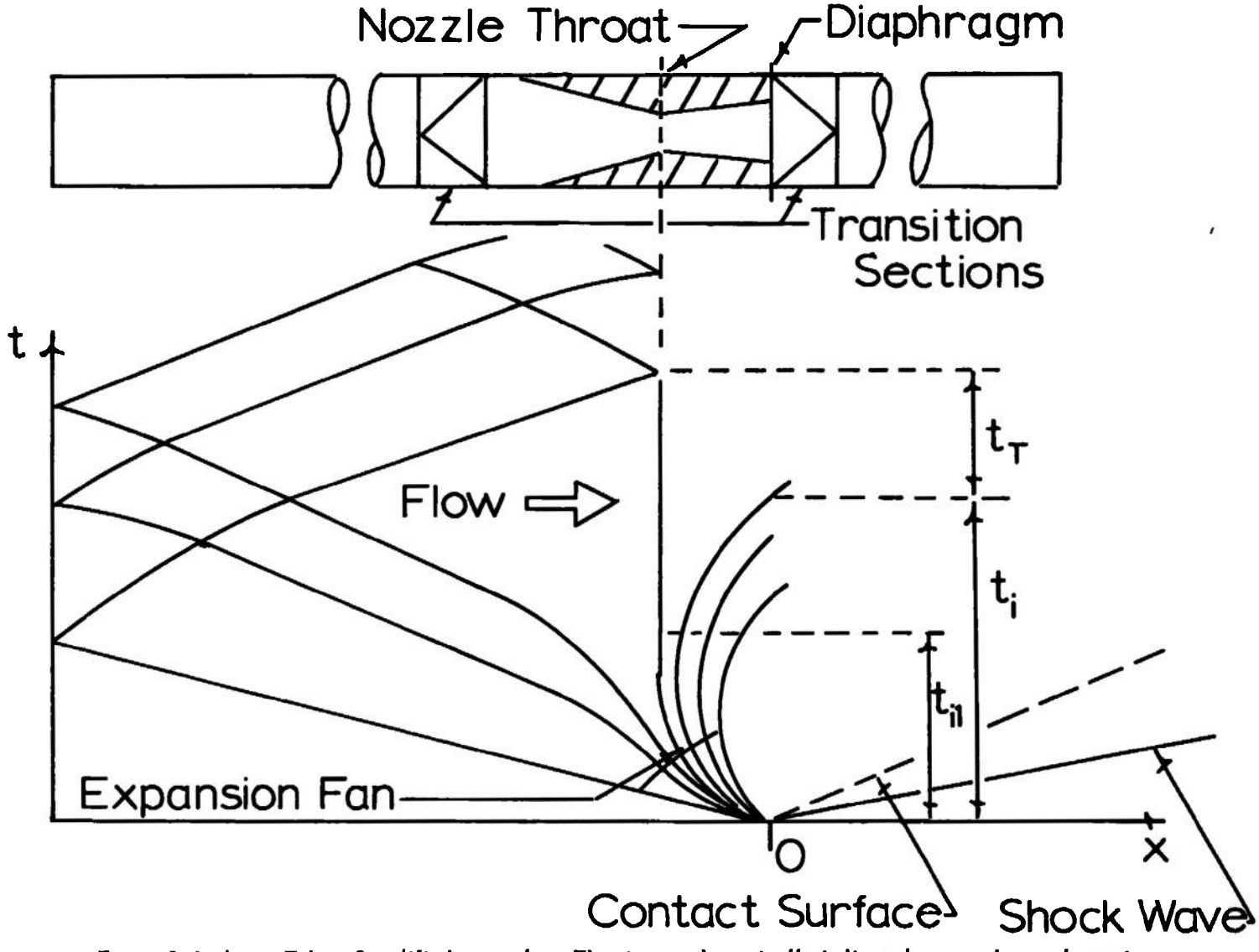

Figure 1 Ludwieg Tube: Simplified t – x plot. The times schematically indicated are t_i, the total starting time; t_{il}, the time required to establish sonic conditions at the nozzle throat; t_T, the totol time of steady supersonic flow.

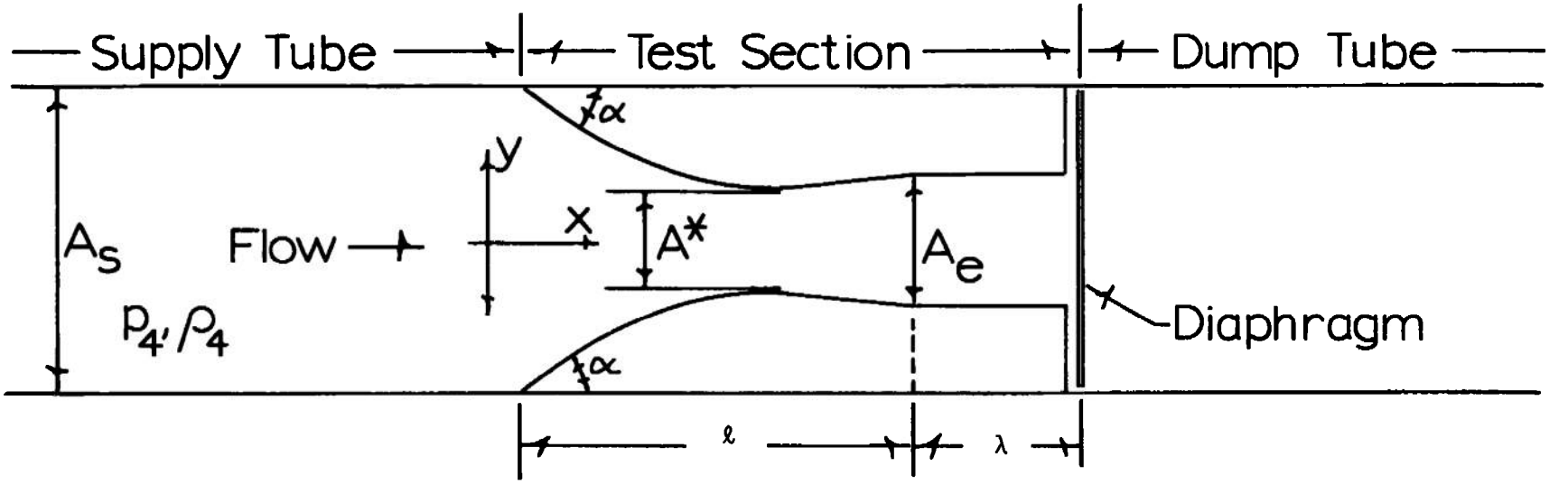

Figure 2 Notation used in the dimensional analysis of the starting flow.

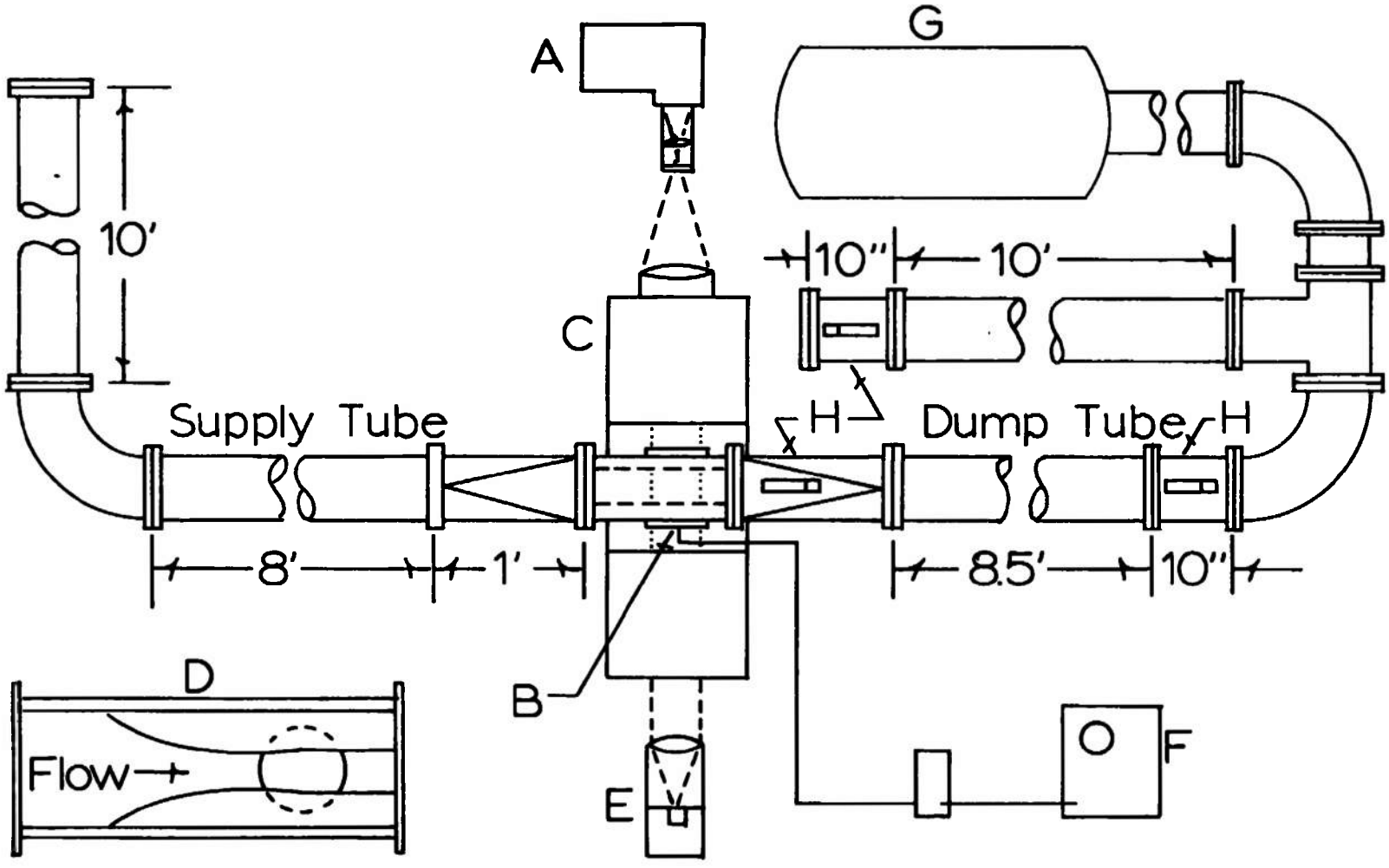

Figure 3 Experimental Apparatus. (A) High speed camera. (B) Pressure transducer at exit position. (C) Mach-Zehnder Interferometer. (D) Side view of 2" x 5" test section with closed jet nozzle in position. (E) Collimating lens and light source. (F) Oscilloscope to record pressure traces. (G) Dump tank, 17 cu ft volume. (H) Diaphragm sections.

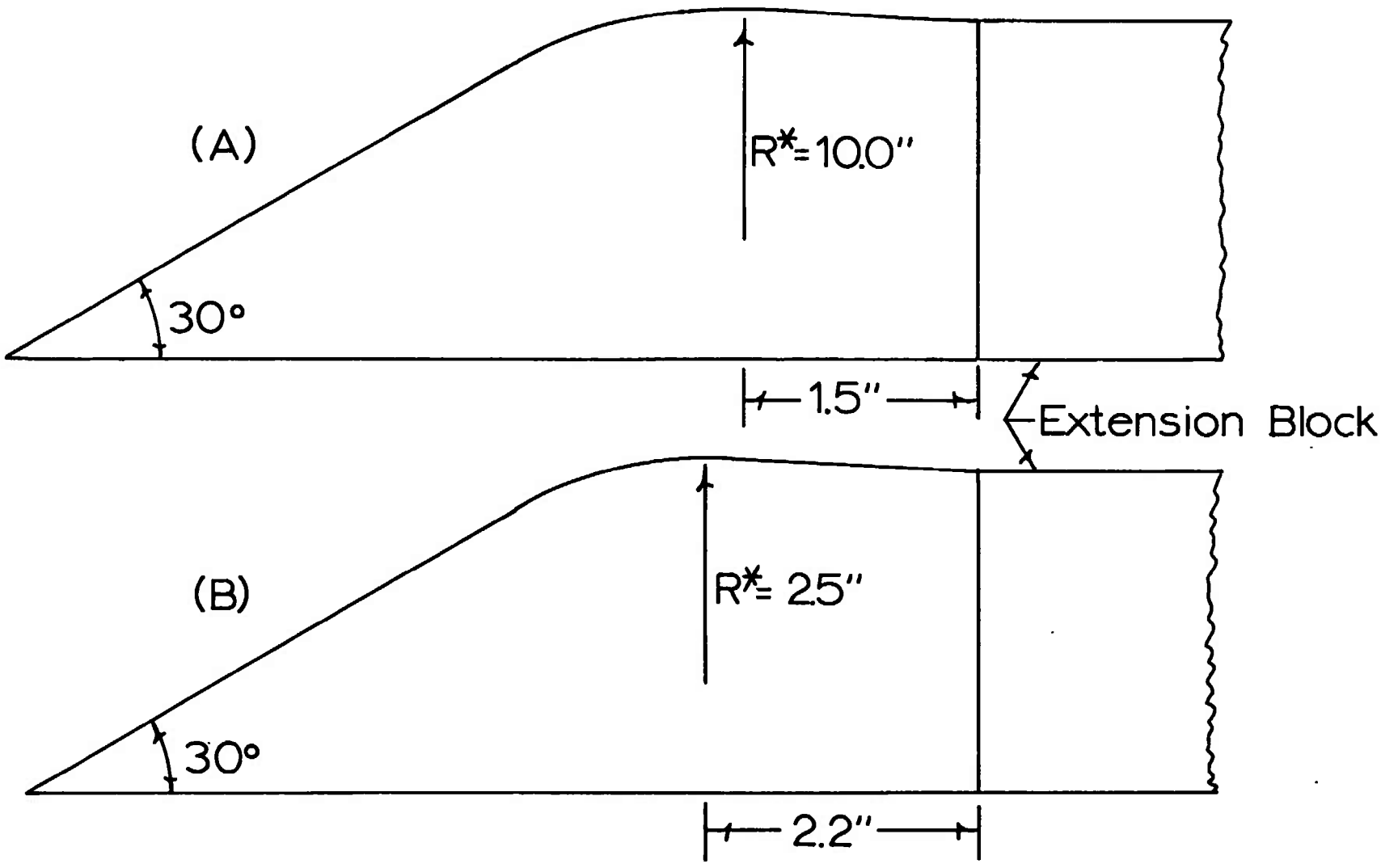

Figure 4 M = 1.6 nozzle profiles. (A) Uniform flow nozzles with a 2.0" x 0.5" throat. (B) Wedge type nozzles.

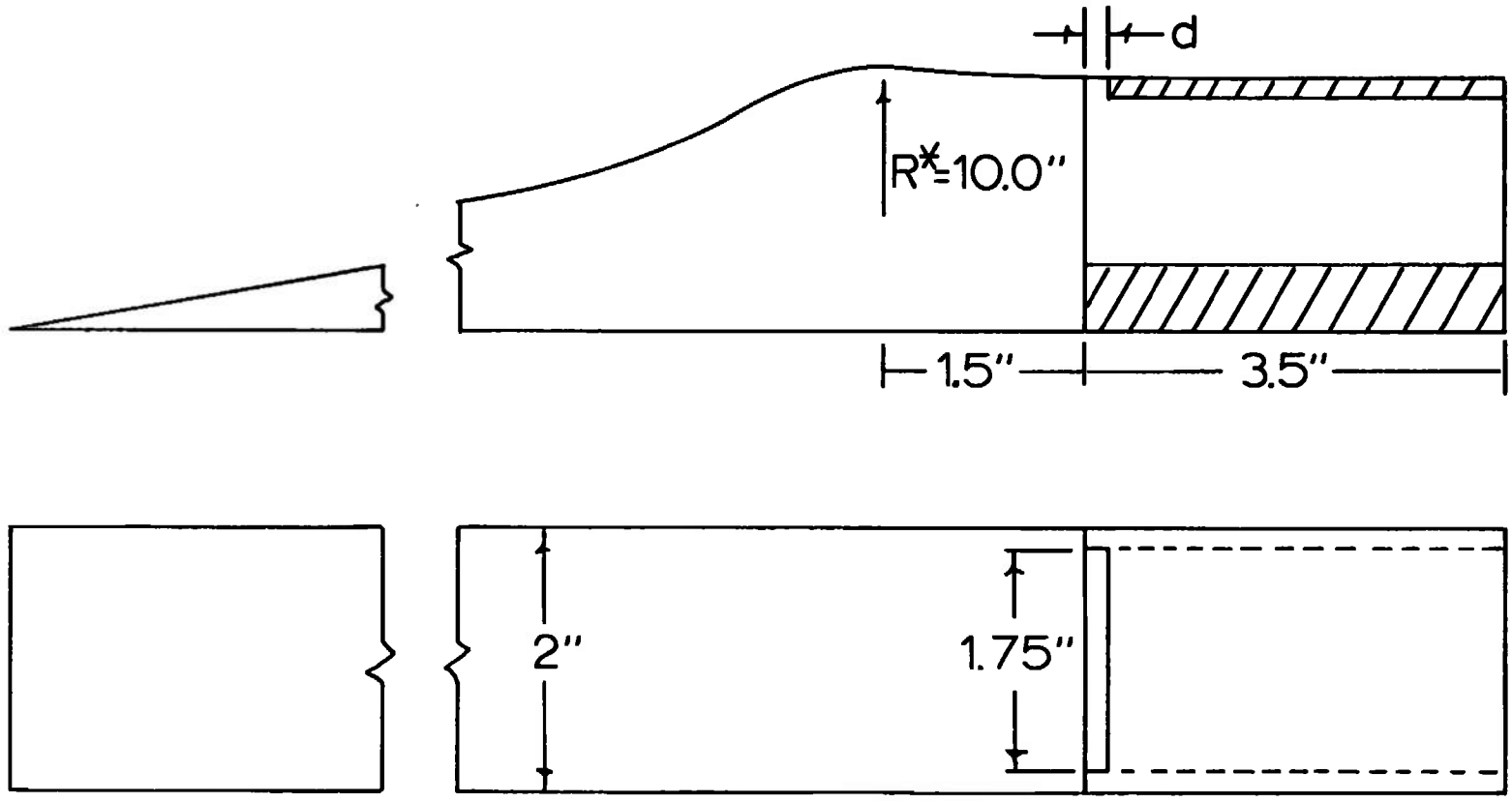

Figure 5 M = 1.6 boundary layer suction nozzle profile. Uniform flow nozzle with a 2.0" x 0.5" throat.

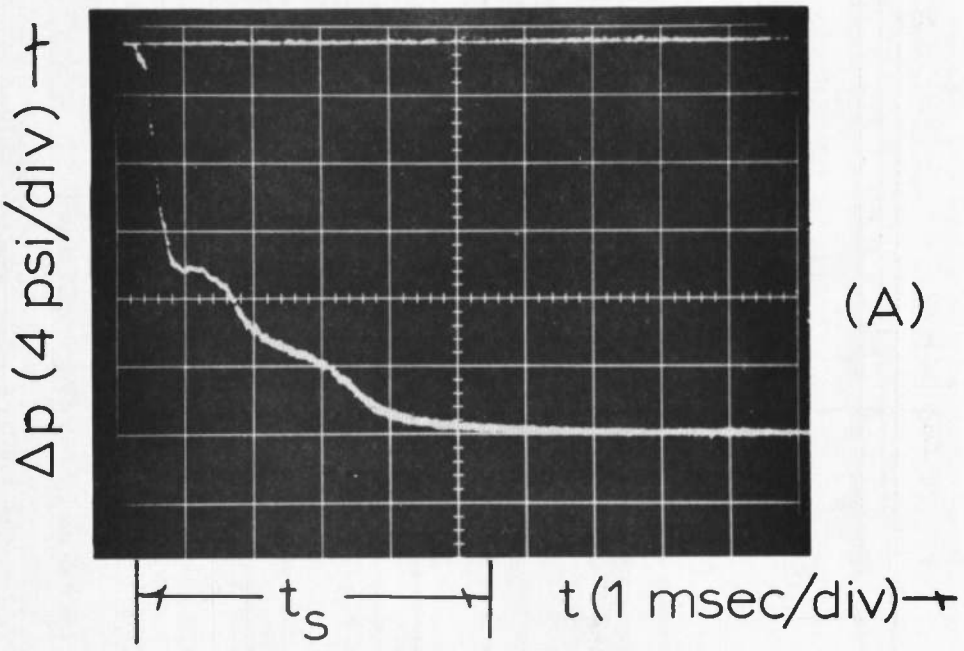

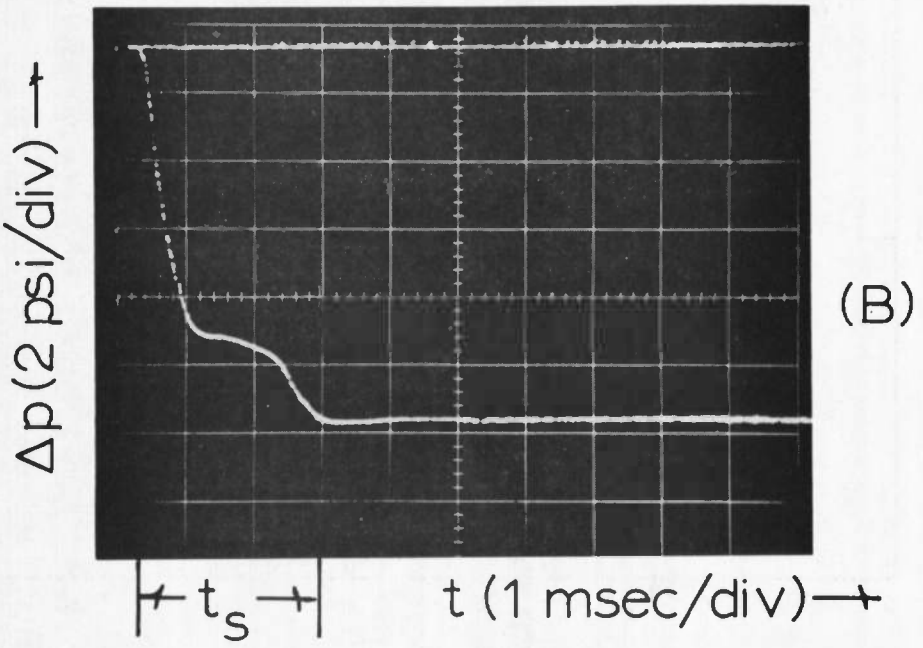

Figure 6 Pressure and starting time measurements. (A) Uniform flow nozzle, $\alpha = 50°$, $A_s/A^* = 22$, $\lambda = 12.7$ cm, $p_4 = 2.0$ atm, $p_4/p_1 = 10$. (B) Wedge type nozzle; $\alpha = 30°$, $A_s/A^* = 8$, $\lambda = 12.7$ cm, $p_4 = 1.0$ atm, $p_4/p_1 = 10^5$. Pressure traces are triggered at diaphragm rupture.

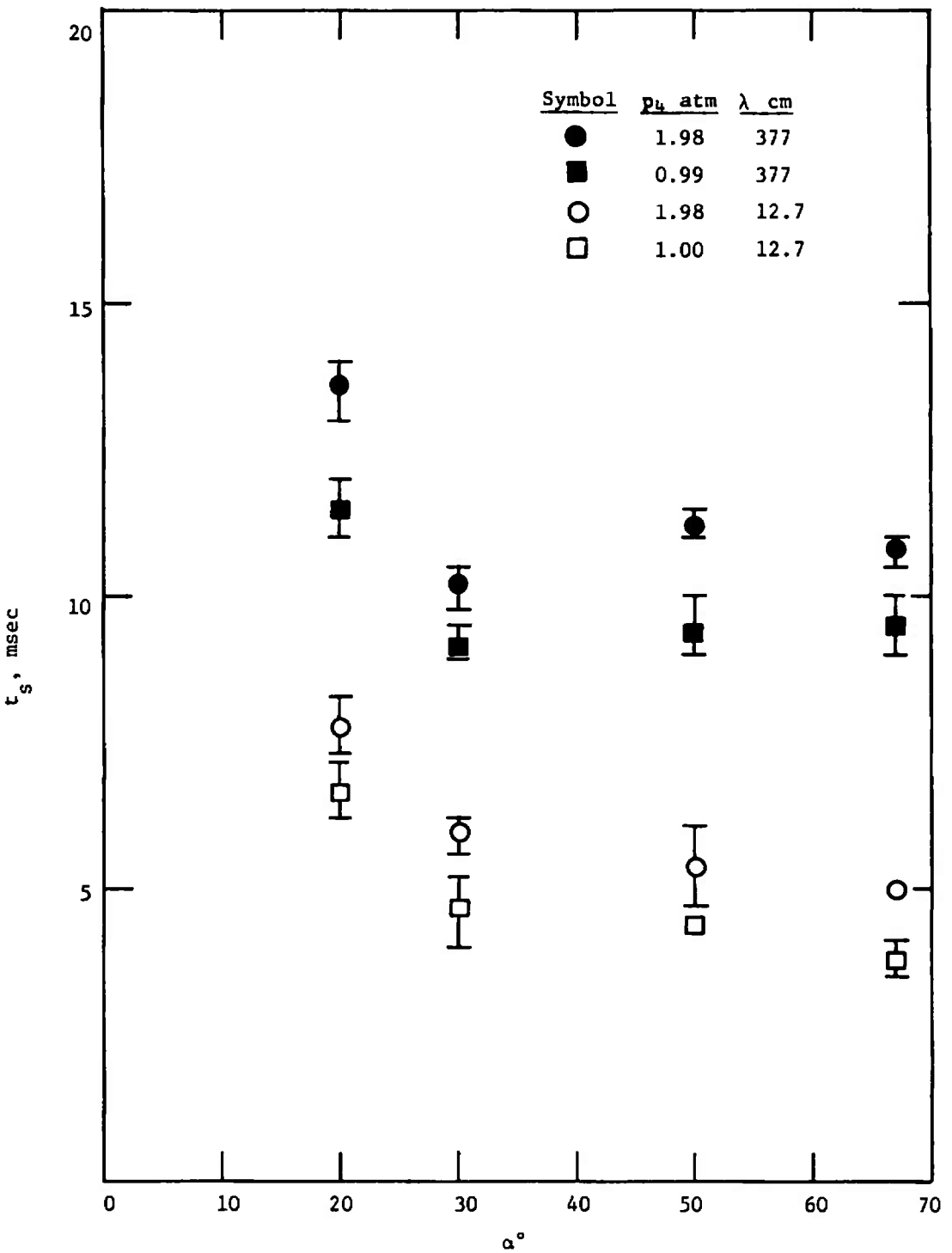

Figure 7 Measured starting time as a function of nozzle inlet angle at fixed contraction ratio, $A_s/A^* = 22$, $p_4/p_1 = 10$, uniform flow nozzles.

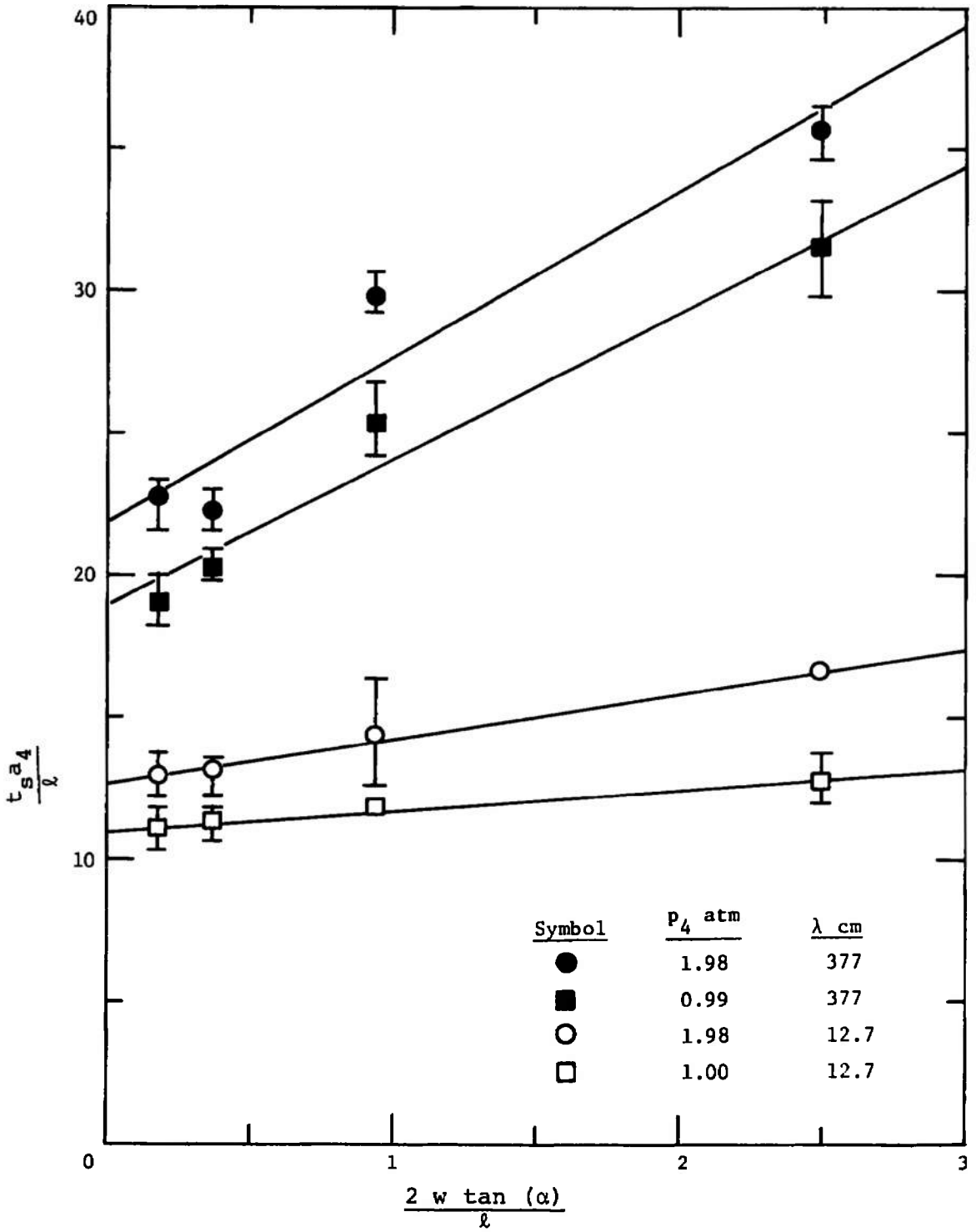

Figure 8 Nondimensional starting time as a function of nondimensional inlet angle at fixed contraction ratio, $A_s/A^* = 22$, $p_4/p_1 = 10$, uniform flow nozzles. Lines shown are obtained from least squares fit of the data.

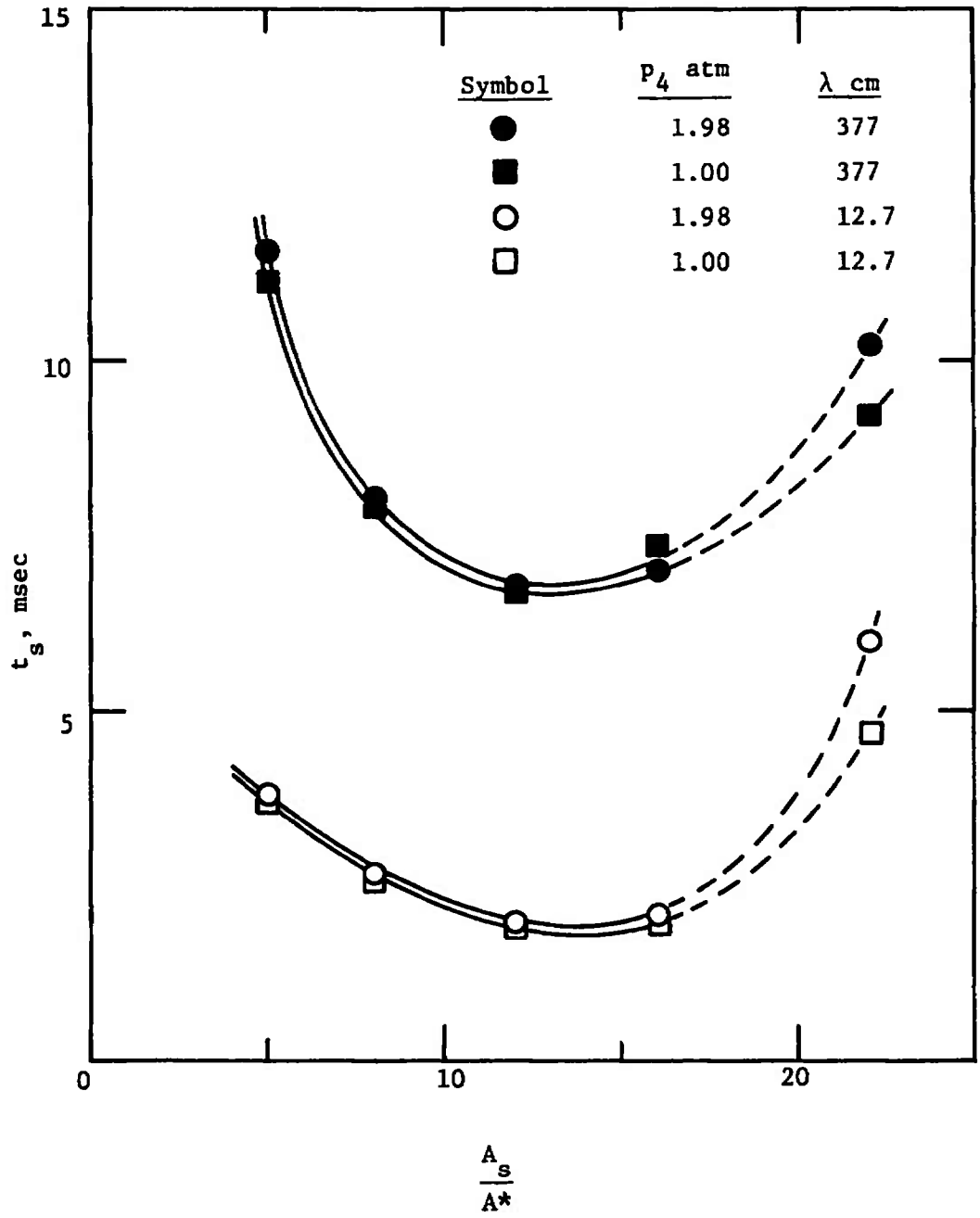

Figure 9 Measured starting time os a function of nozzle contraction rotio at fixed inlet ongle, $\alpha = 30°$, $p_4/p_1 = 10$. A smoath curve connects the data, with the dashed section representing the change from wedge type to uniform flow nozzle geometry ($A_s/A^* = 22$).

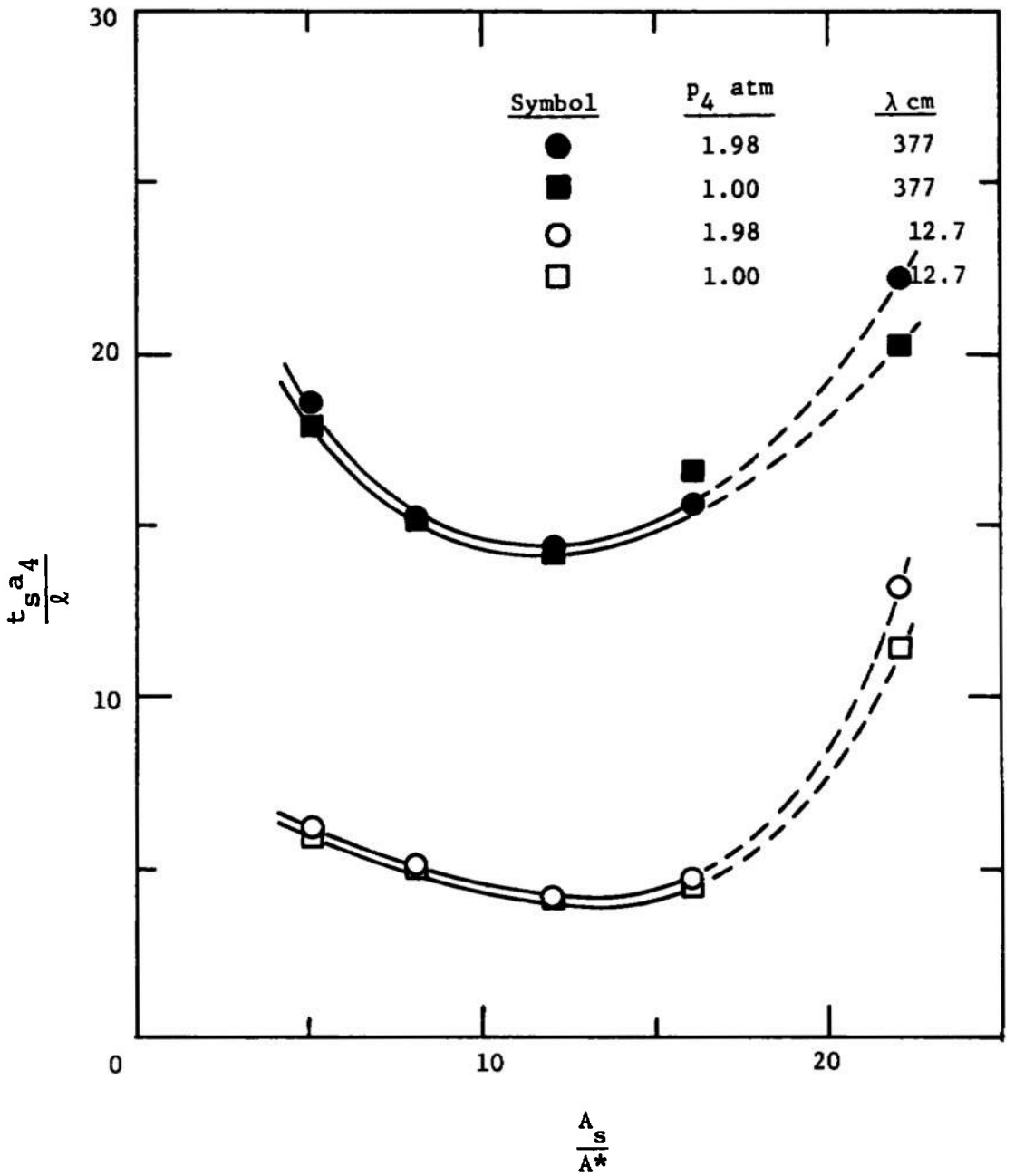

Figure 10 Nondimensional starting time as a function of nozzle contraction ratio at fixed inlet angle, $\alpha = 30°$, $p_4/p_1 = 10$. A smooth curve connects the data, with the dashed section representing the change from wedge type to uniform flow nozzle geometry ($A_s/A^* = 22$).

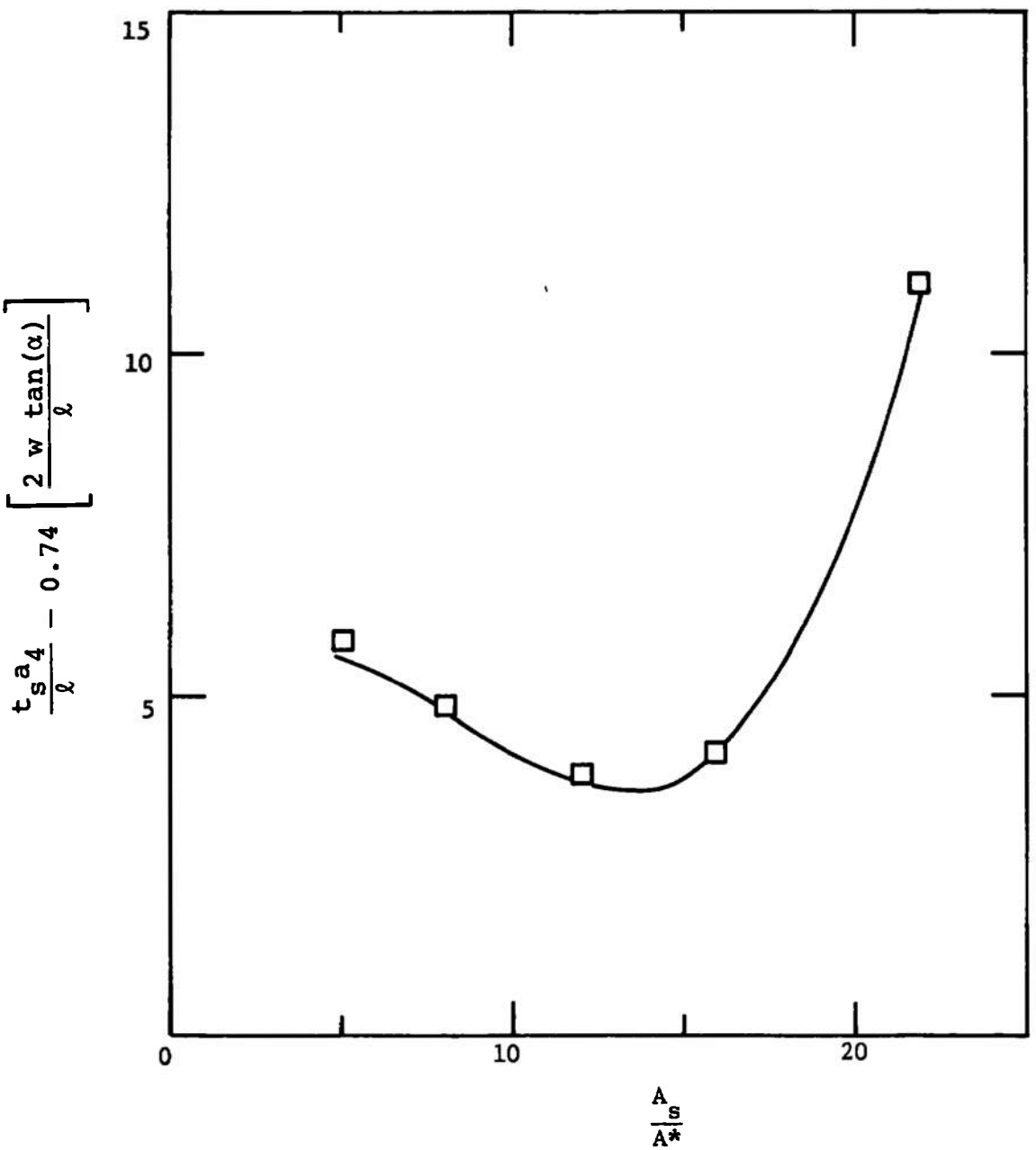

Figure 11 Correlation of the results obtained in uniform flow and wedge nozzle experiments p_4 = 1.0 atm, p_4/p_1 = 10, λ = 12.7 cm, 20° ≤ α ≤ 67°, 10 cm ≤ ℓ ≤ 21 cm. Fitted curve represents a cubic expression in A_s/A^*.

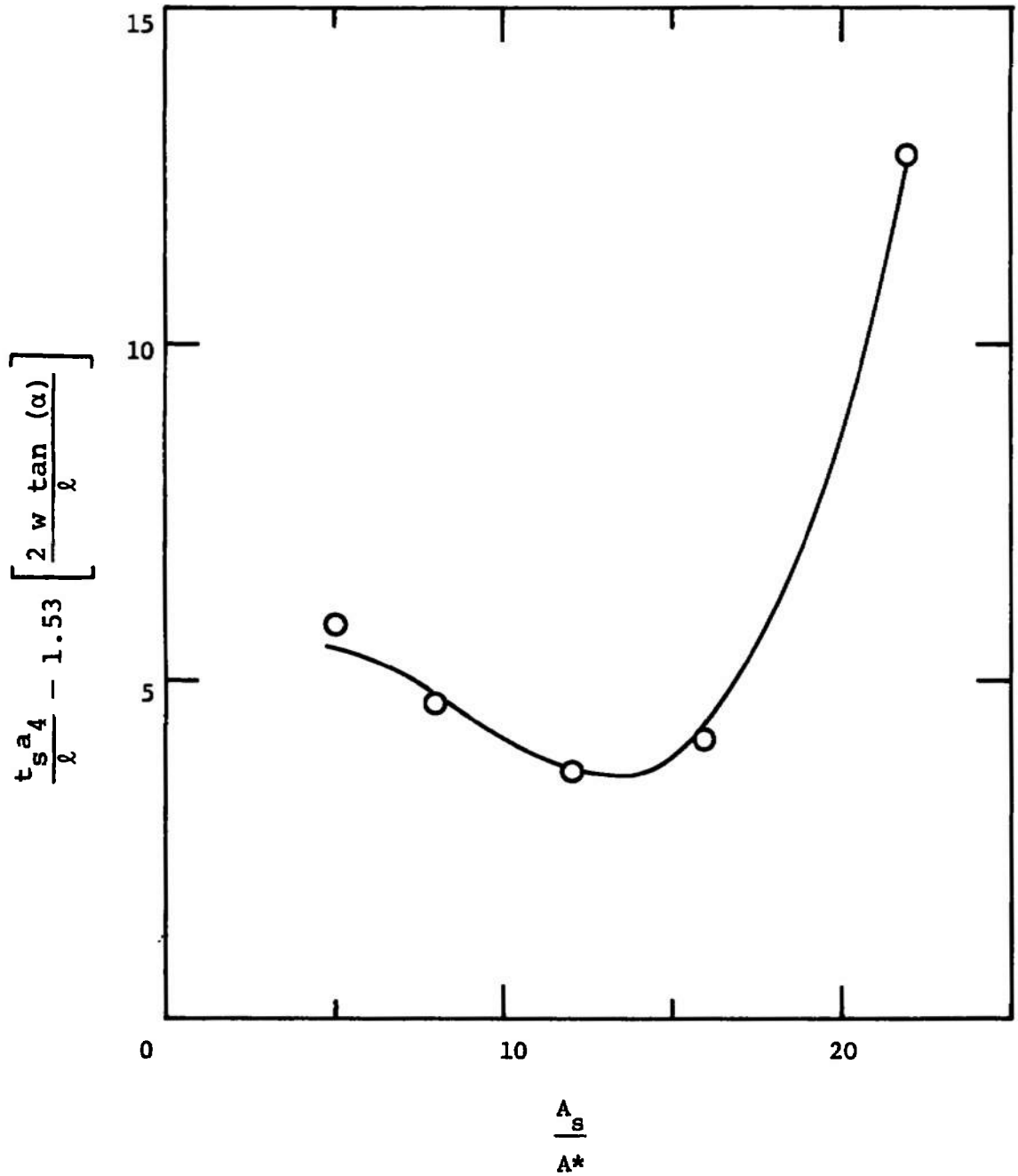

Figure 12 Correlation of the results obtained in uniform flow and wedge nozzle experiments. $p_4 = 2.0$ atm, $p_4/p_1 = 10$, $\lambda = 12.7$ cm, $20° \leq \alpha \leq 67°$, 10 cm $\leq \ell \leq 21$ cm. Fitted curve represents a cubic expression in A_s/A^*.

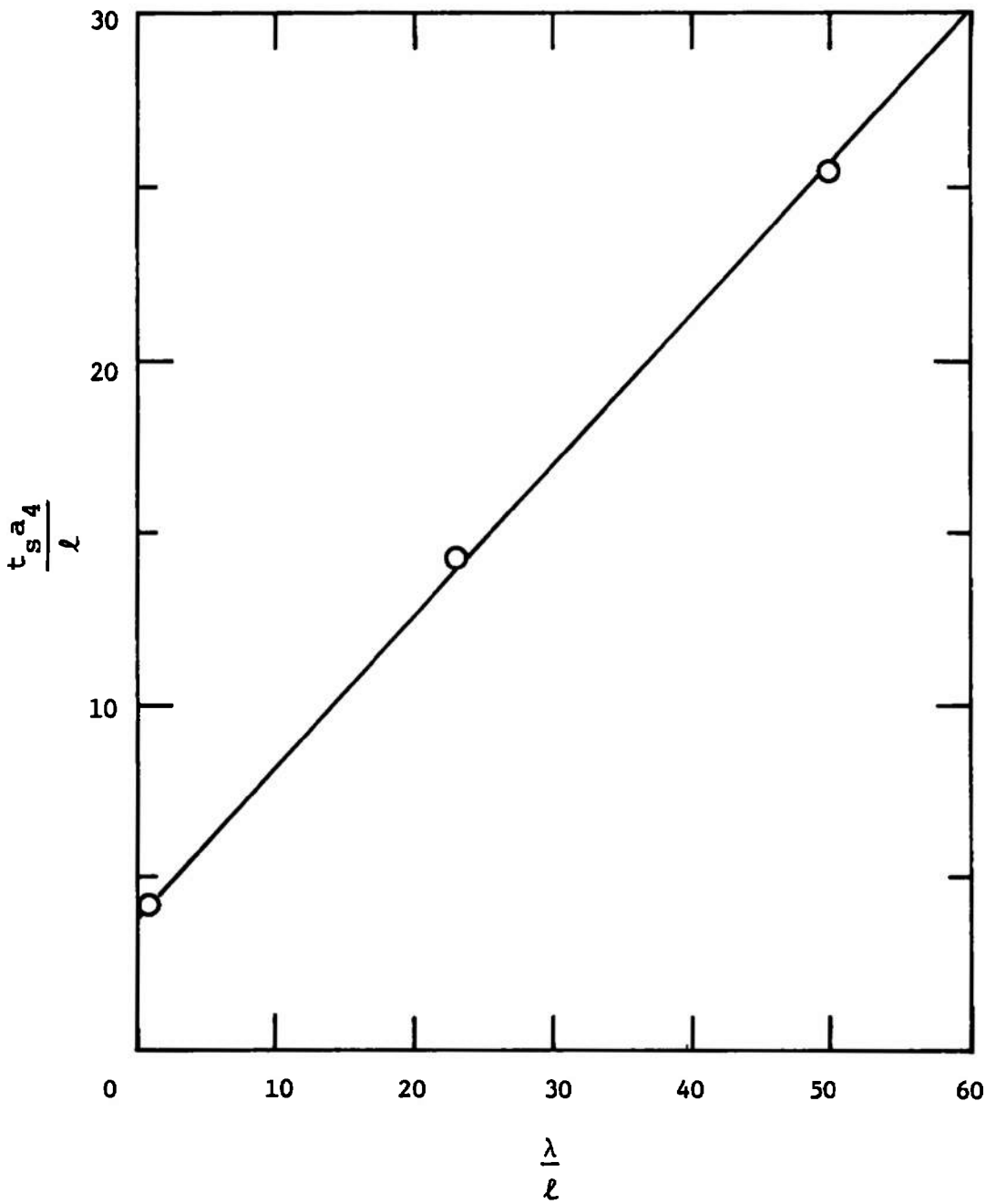

Figure 13 Measured nondimensional starting time as a function of nondimensional distance to the downstream diaphragm location. p_4 = 3 atm, p_4/p_1 = 3, ℓ = 16.4 cm, α = 30°, A_s/A^* = 12, wedge type nozzle.

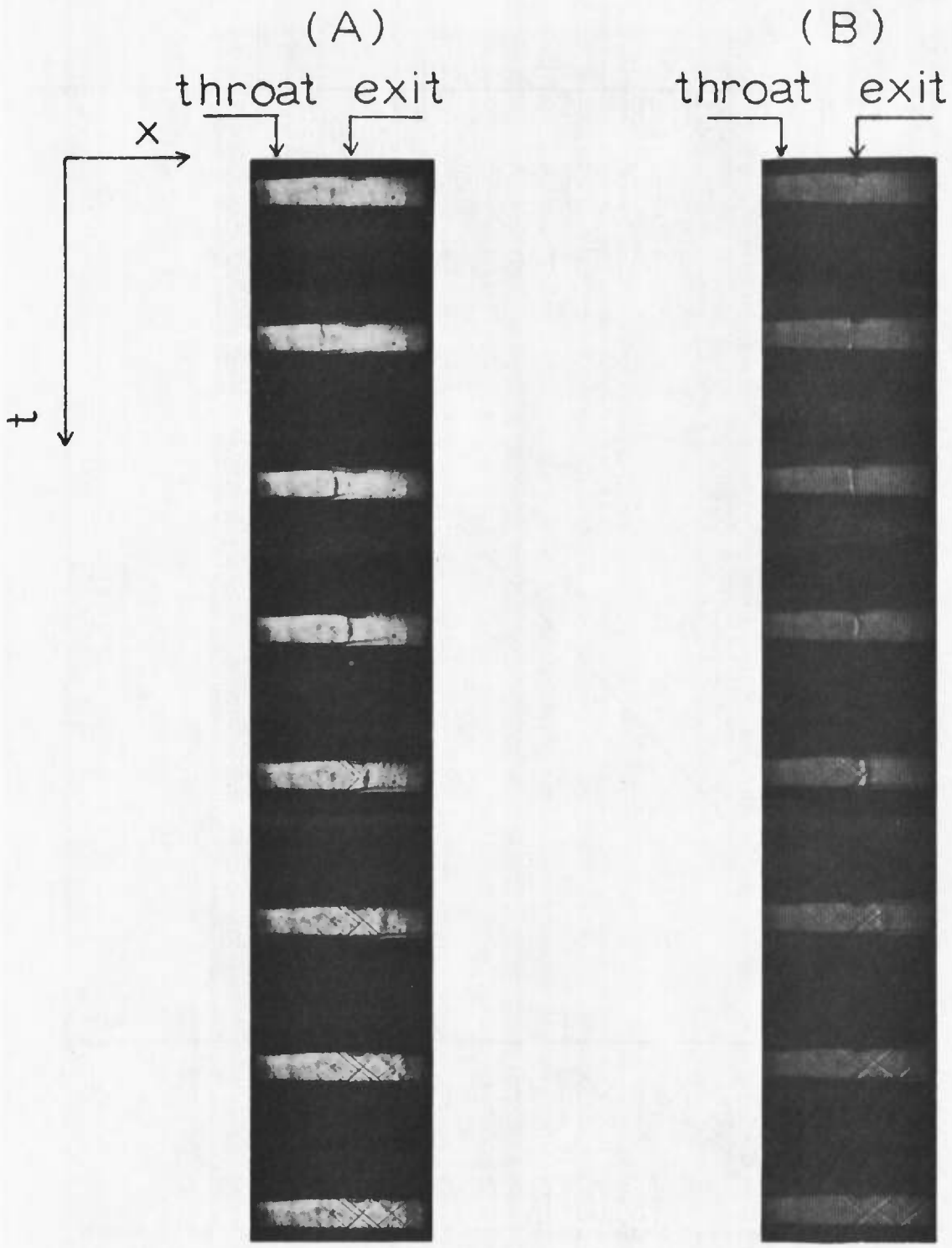

Figure 14 Shadowgroph high speed movie prints of the starting process in the closed jet, uniform flow nozzle. (A) without boundory loyer suction, (B) with boundary layer suction, suction slit dimensions 1.75" x 0.200". The time between eoch frame is obout 0.2 msec; field of view shows nozzle throot ot left, nozzle exit ond slit locotion in center. Flow is from left to right. $p_4 = 2.0$ otm, $p_4/p_1 = 10$, $\lambda = 12.7$ cm.

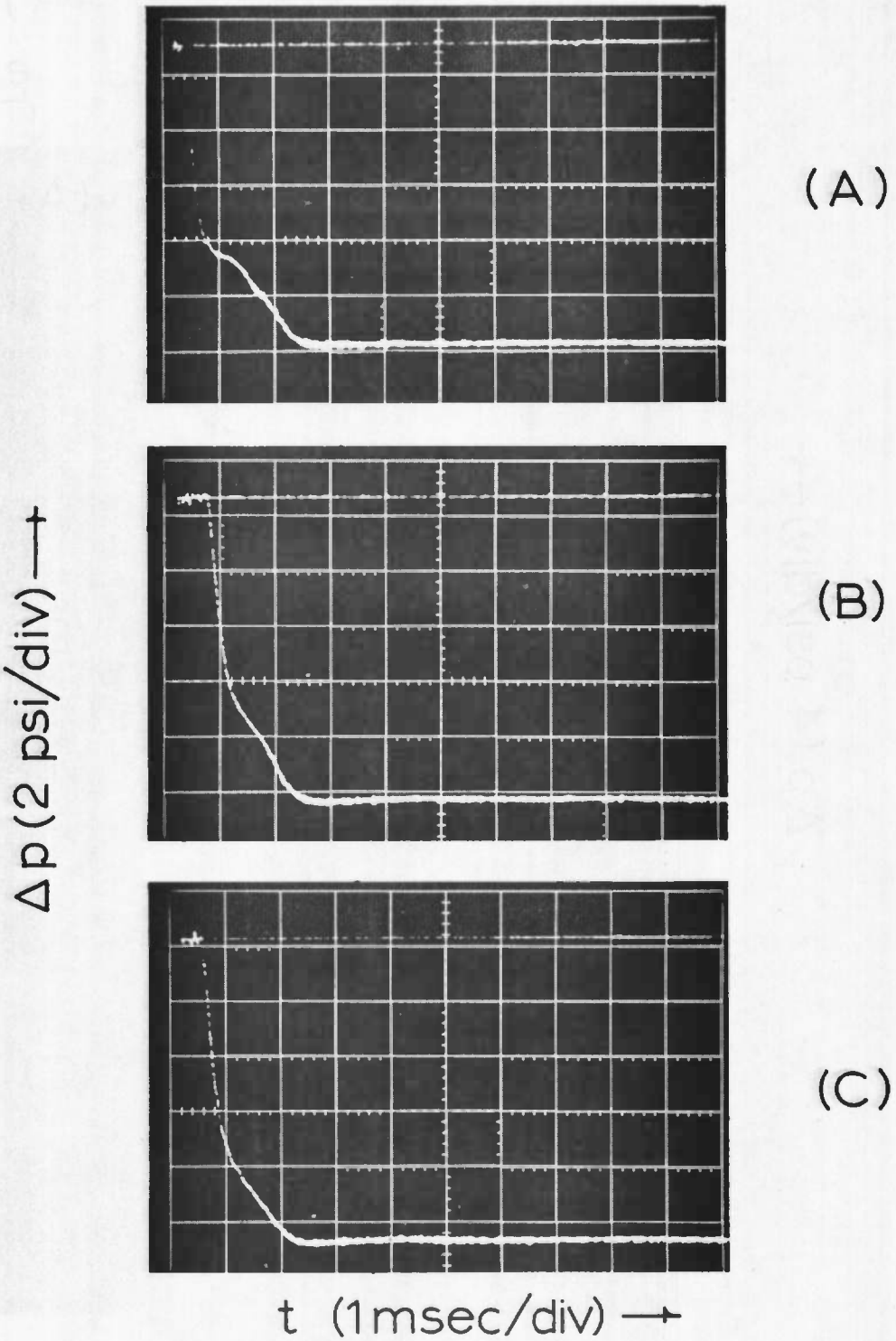

Figure 15 Static pressure traces with and without boundary layer suction at p_4 = 1.0 atm, p_4/p_1 = 10, λ = 12.7 cm. (A) No suction. (B) 1.75" x 0.060" suction slit. (C) 1.75" x 0.200" suction slit. Pressure traces are triggered at diaphragm rupture.

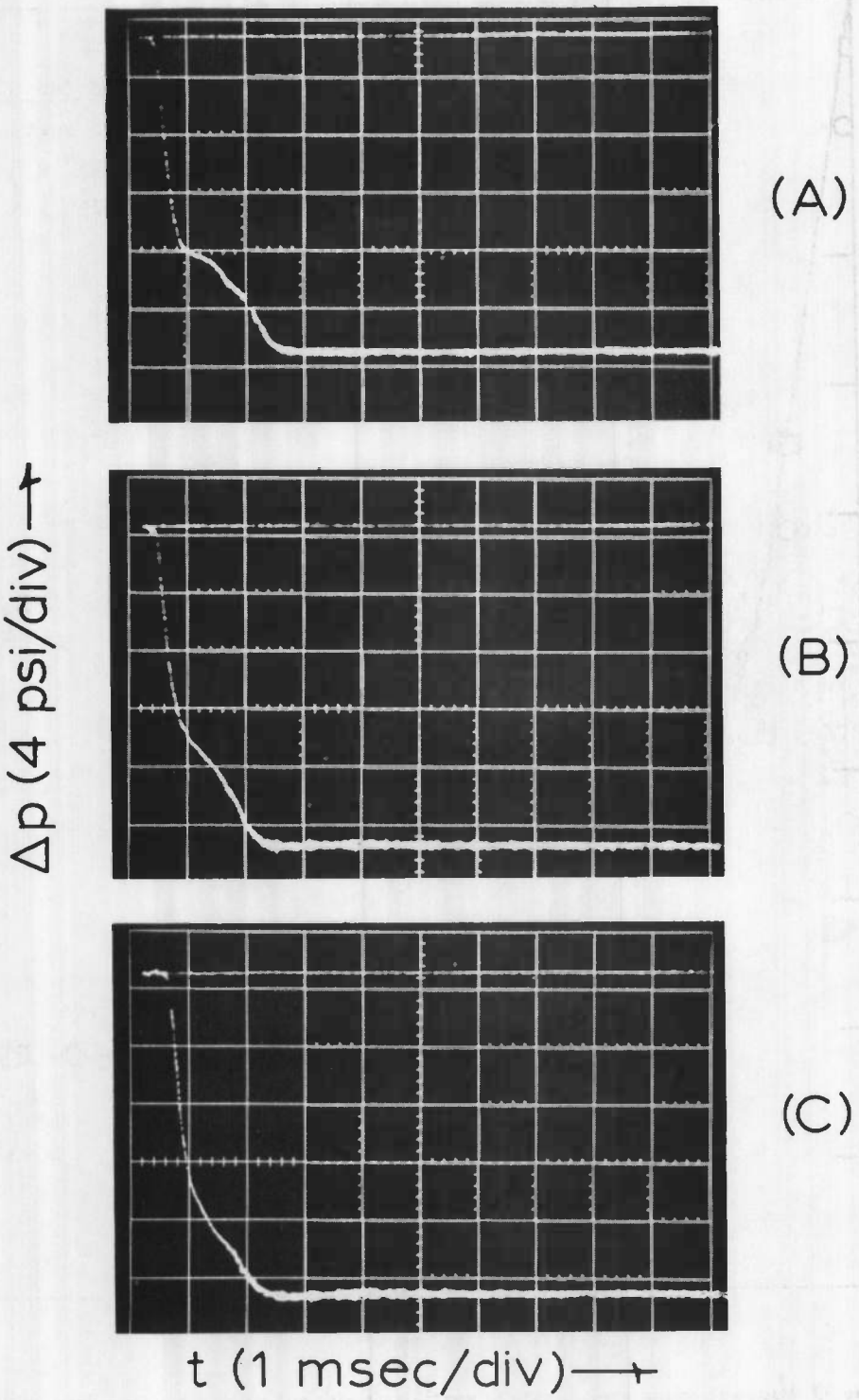

Figure 16 Static pressure traces with and without boundory loyer suction at p_4 = 2.0 atm, p_4/p_1 = 10, λ = 12.7 cm. (A) No suction. (B) 1.75" x 0.060" suction slit. (C) 1.75" x 0.200" suction slit. Pressure traces are triggered at diophrogm rupture.

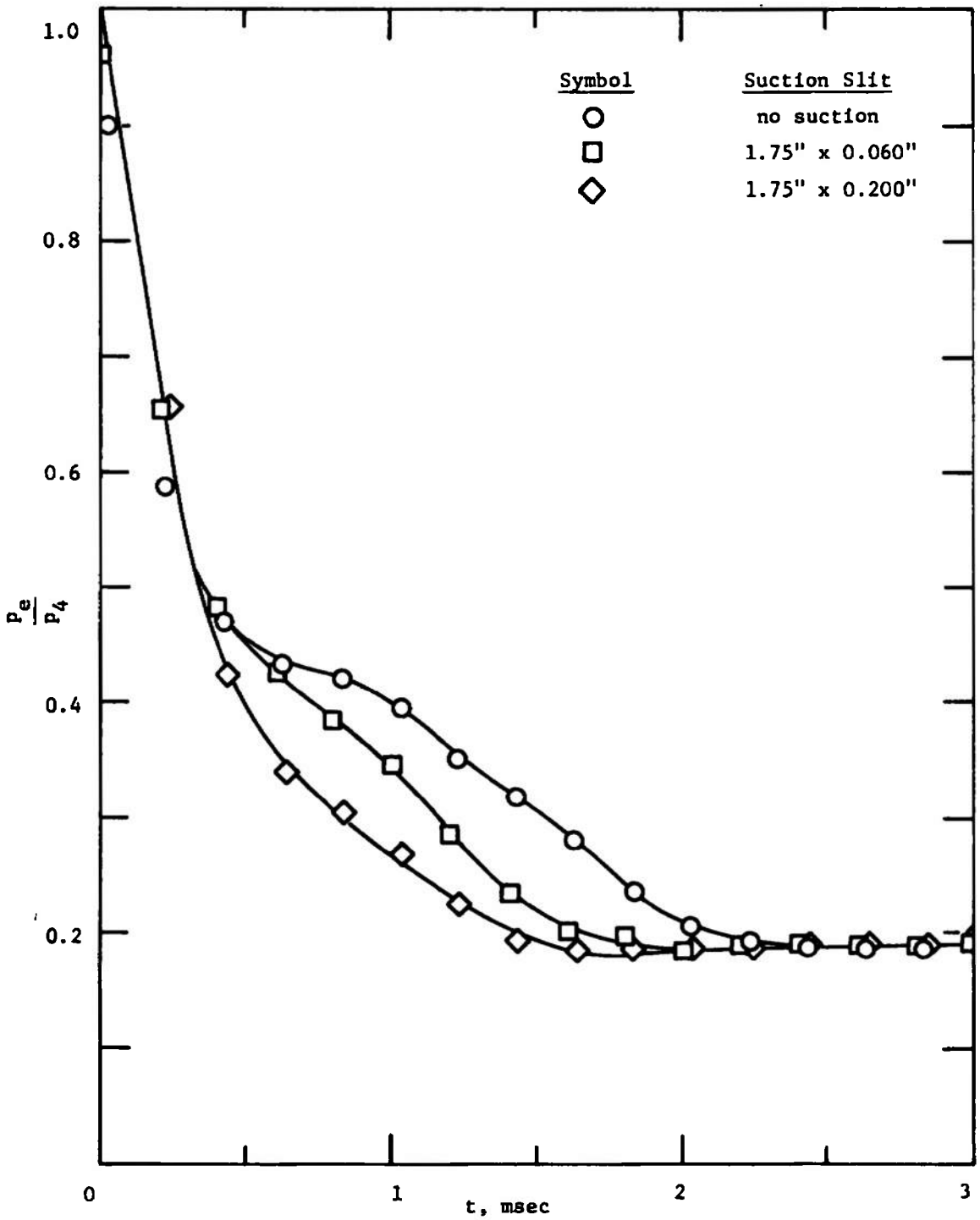

Figure 17 Measured stotic pressure at the nozzle exit with and without boundary layer suction. p_4 = 1.0 atm, p_4/p_3 = 10, λ = 12.7 cm. Time starts with the arrival of the expansion wave at the exit.

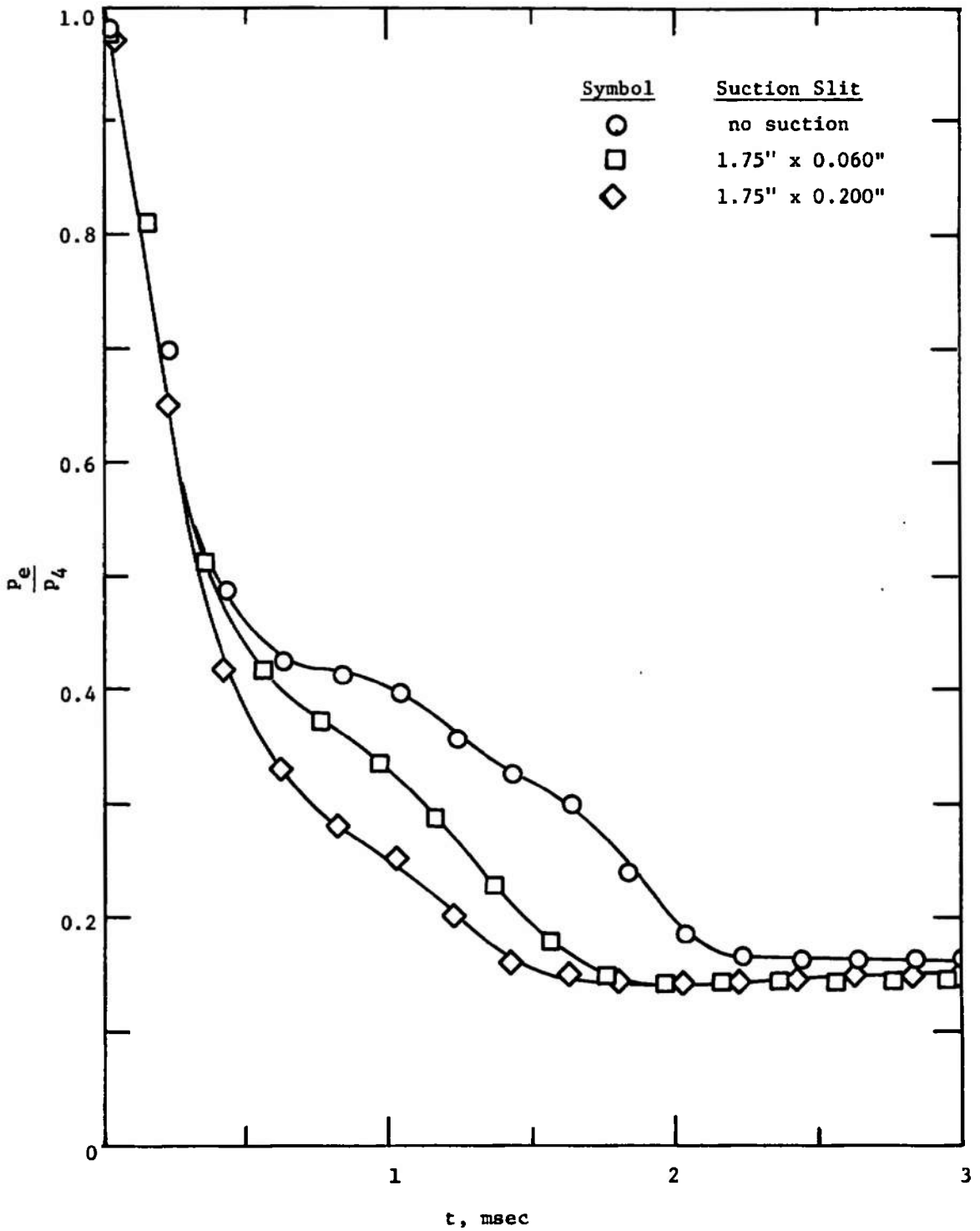

Figure 18 Measured static pressure at the nozzle exit with and without boundary layer suction. $p_4 = 2.0$ atm, $p_4/p_1 = 10$, $\lambda = 12.7$ cm. Time starts with the arrival of the expansion wave at the exit.

UNCLASSIFIED

Security Classification

DOCUMENT CONTROL DATA - R & D

(Security classification of title, body of abstract and indexing annotation must be entered when the overall report is classified)

1 ORIGINATING ACTIVITY *(Corporate author)*
Yale University
New Haven, Connecticut 06520

2a. REPORT SECURITY CLASSIFICATION
UNCLASSIFIED

2b. GROUP
N/A

3 REPORT TITLE
EFFECTS OF NOZZLE GEOMETRY AND DIAPHRAGM LOCATION ON THE STARTING PROCESS IN A LUDWIEG TUBE

4 DESCRIPTIVE NOTES *(Type of report and inclusive dates)*
Final Report - July 1971 to June 1972

5 AUTHOR(S) *(First name, middle initial, last name)*
Leo T. Smith and Francis Mosnier

6 REPORT DATE	7a. TOTAL NO. OF PAGES	7b. NO OF REFS
February 1973	49	14

8a. CONTRACT OR GRANT NO	9a. ORIGINATOR'S REPORT NUMBER(S)
b. PROJECT NO	AEDC-TR-73-21
c. Program Element 65802F	9b. OTHER REPORT NO(S) *(Any other numbers that may be assigned this report)*
d.	N/A

10 DISTRIBUTION STATEMENT
Approved for public release; distribution unlimited.

11 SUPPLEMENTARY NOTES	12 SPONSORING MILITARY ACTIVITY
Available in DDC	Arnold Engineering Development Center, Air Force Systems Command, Arnold AF Station, TN 37389

13 ABSTRACT

The starting process in the Ludwieg tube, an intermittent type wind tunnel, was experimentally investigated. Starting flow with varying initial supply gas pressure, nozzle geometry, and downstream diaphragm location, was studied. Two types of closed jet nozzle configurations were used: uniform flow M = 1.6 nozzles, and wedge type M = 1.6 nozzles. Dry air at 1, 2, and 3 atm pressure and room temperature served as the test gas. Starting times were determined from static pressure recordings, made at the exit of the nozzle, and the presence or absence of starting shock waves was confirmed by high speed shadowgraph films of the flow. A dimensional analysis that relates nozzle starting time to the supply conditions, nozzle inlet angle, nozzle contraction ratio, and distance to the diaphragm was performed, and it was found to correlate the measurements. For all combinations of supply conditions, nozzle geometry, and diaphragm location treated, starting shock waves were observed in the nozzle. These shocks were eliminated and steady supersonic flow was established smoothly throughout the closed jet nozzle by applying boundary layer suction at the exit.

DD FORM 1 NOV 65 1473

UNCLASSIFIED

Security Classification

14. KEY WORDS	LINK A		LINK B		LINK C	
	ROLE	WT	ROLE	WT	ROLE	WT
Ludwieg tubes						
wind tunnels						
supersonic flow						
nozzles						
diaphragm location						